Behavioral/Cognitive

Corticostriatal Suppression of Appetitive Pavlovian Conditioned Responding

Franz R. Villaruel, Melissa Martins, and Nadia Chaudhri†
Center for Studies in Behavioral Neurobiology, Department of Psychology, Concordia University, Montreal, Quebec H4B 1R6, Canada

The capacity to suppress learned responses is essential for animals to adapt in dynamic environments. Extinction is a process by which animals learn to suppress conditioned responding when an expected outcome is omitted. The infralimbic (IL) cortex to nucleus accumbens shell (NAcS) neural circuit is implicated in suppressing conditioned responding after extinction, especially in the context of operant cocaine-seeking behavior. However, the role of the IL-to-NAcS neural circuit in the extinction of responding to appetitive Pavlovian cues is unknown, and the psychological mechanisms involved in response suppression following extinction are unclear. We trained male Long Evans rats to associate a 10 s auditory conditioned stimulus (CS; 14 trials per session) with a sucrose unconditioned stimulus (US; 0.2 ml per CS) in a specific context, and then following extinction in a different context, precipitated a renewal of CS responding by presenting the CS alone in the original Pavlovian conditioning context. Unilateral, optogenetic stimulation of the IL-to-NAcS circuit selectively during CS trials suppressed renewal. In a separate experiment, IL-to-NAcS stimulation suppressed CS responding regardless of prior extinction and impaired extinction retrieval. Finally, IL-to-NAcS stimulation during the CS did not suppress the acquisition of Pavlovian conditioning but was required for the subsequent expression of CS responding. These results are consistent with multiple studies showing that the IL-to-NAcS neural circuit is involved in the suppression of operant cocaine-seeking, extending these findings to appetitive Pavlovian cues. The suppression of appetitive Pavlovian responding following IL-to-NAcS circuit stimulation, however, does not appear to be an extinction-dependent process.

Key words: **extinction; infralimbic cortex; nucleus accumbens; optogenetics; Pavlovian conditioning; ventromedial prefrontal cortex**

Significance Statement

Extinction is a form of inhibitory learning through which animals learn to suppress conditioned responding in the face of nonreinforcement. We investigated the role of the IL cortex inputs to the NAcS in the extinction of responding to appetitive Pavlovian cues and the psychological mechanisms involved in response suppression following extinction. Using *in vivo* optogenetics, we found that stimulating the IL-to-NAcS neural circuit suppressed context-induced renewal of conditioned responding after extinction. In a separate experiment, stimulating the IL-to-NAcS circuit suppressed conditioned responding in an extinction-independent manner. These findings can be used by future research aimed at understanding how corticostriatal circuits contribute to behavioral flexibility and mental disorders that involve the suppression of learned behaviors.

Received Aug. 16, 2021; revised Sep. 29, 2021; accepted Oct. 9, 2021.

Author contributions: F.R.V. and N.C. designed research; F.R.V. and M.M. performed research; F.R.V., M.M., and N.C. analyzed data; F.R.V. and N.C. wrote the paper.

This work was supported by the Natural Sciences and Engineering Research Council of Canada Grant 387 224-2010 (to N.C.) and a Chercheur-Boursier Junior 2 Award from Fonds de Recherche du Québec–Santé (to N.C.). F.R.V. was supported by graduate fellowships from Concordia University and the Natural Sciences and Engineering Research Council of Canada. We thank Steve Cabilio for support with Med-PC programming and data extraction, David Munro for technical support, and Dr. Chris Law of the Center for Microscopy and Cellular Imaging for writing the Fiji macro and programs for Fos and tracer quantification and technical support in microscopy.

This paper is dedicated to Nadia Chaudhri (N.C.) who passed away from ovarian cancer on October 5, 2021. In memory of her tremendous mentorship and scientific contributions.

†Deceased, Oct. 5, 2021.

The authors declare no competing financial interests.

Correspondence should be addressed to Franz R. Villaruel at fr.villaruel@gmail.com.

https://doi.org/10.1523/JNEUROSCI.1664-21.2021

Introduction

The capacity to inhibit learned responses is essential for adaptive behavior. Extinction is a fundamental psychological process by which animals learn to suppress responding to a conditioned stimulus (CS) that previously predicted a biologically significant unconditioned stimulus (US). New inhibitory learning is thought to occur during extinction when the CS is presented without the anticipated US (Konorski, 1948; Pearce and Hall, 1980). Following extinction, retrieval of this inhibitory memory suppresses conditioned responding. However, retrieval of the inhibitory extinction memory is context dependent, and a renewal of conditioned responding can occur when the context is changed after extinction (Bouton, 1993, 2004). This impermanence of response suppression is a fundamental shortcoming in using

extinction to treat disorders such as post-traumatic stress and substance abuse, which are characterized by heightened responses to environmental cues.

The infralimbic (IL) medial prefrontal cortex is a critical brain region for extinction (Quirk et al., 2000; Milad and Quirk, 2002; Rhodes and Killcross, 2004, 2007; Vidal-Gonzalez et al., 2006; Peters et al., 2008, 2009; Quirk and Mueller, 2008; LaLumiere et al., 2012; Do-Monte et al., 2015; Gutman et al., 2017; Villaruel et al., 2018; Lay et al., 2019) and is thought to mediate the extinction of appetitive and aversive conditioning through distinct projections to the nucleus accumbens shell (NAcS) and the basolateral amygdala (BLA), respectively (Peters et al., 2009; Bloodgood et al., 2018). Studies on the IL-to-NAcS neural circuit in appetitive extinction typically involve instrumental conditioning in which animals make an operant response to earn drug reinforcers. Pharmacologically disconnecting the IL and the NAcS reinstates extinguished cocaine-seeking (Peters et al., 2008), whereas promoting glutamatergic transmission between the IL and NAcS suppresses cocaine-seeking (LaLumiere et al., 2012). Furthermore, chemogenetic stimulation of the IL-to-NAcS circuit reduces cue-induced cocaine-seeking (Augur et al., 2016). These results suggest that activity in the IL-to-NAcS circuit suppresses operant cocaine-seeking after extinction. Finally, pharmacological disconnection of the IL and NAcS disrupts the capacity of a Pavlovian cue to invigorate operant responding, suggesting that the circuit is also involved in processing appetitive Pavlovian associations (Keistler et al., 2015). However, little is known about the role of the IL-to-NAcS neural circuit explicitly in extinction of appetitive Pavlovian conditioned responding.

The IL and NAcS may mediate the suppression of conditioned responding by facilitating the retrieval of an inhibitory extinction memory. Extinction increases IL activity (Milad and Quirk, 2002) and induces synaptic plasticity in the NAcS (Sutton et al., 2003). In aversive conditioning, pharmacologically stimulating the IL strengthens inhibitory memory and facilitates extinction retrieval (Lingawi et al., 2017, 2018). Furthermore, distinct neuronal ensembles that mediate extinction of cocaine-seeking exist within the IL and IL-to-NAcS circuit (Warren et al., 2016; 2019). In some studies, extinction is a prerequisite for IL and IL-to-NAcS stimulation to suppress operant cocaine-seeking (Augur et al., 2016; Müller Ewald et al., 2019). However, optogenetic stimulation of the IL and IL-to-NAcS circuit can also suppress operant food-seeking and cocaine-seeking without prior extinction training (Do-Monte et al., 2015; Cameron et al., 2019). Therefore, it remains unclear if the IL-to-NAcS circuit suppresses responding through the retrieval and strengthening of an extinction memory, especially in appetitive conditioning.

Here, we examined the role of the IL-to-NAcS neural circuit in the suppression of appetitive Pavlovian conditioned responding after extinction. First, we tested whether optogenetic stimulation of the IL-to-NAcS circuit during presentations of a sucrose-predictive CS would suppress context-induced renewal of conditioned responding. In a supplementary experiment, we tested whether activation of the IL-to-BLA circuit would also attenuate renewal. Second, we adapted a procedure from Lingawi et al. (2017) to determine whether the suppression of conditioned responding was because of the retrieval of an inhibitory extinction memory that recruited the IL-to-NAcS neural circuit. Finally, to determine whether stimulating this circuit nonspecifically reduces behavior, we investigated the effect of IL-to-NAcS stimulation on acquisition and expression of appetitive Pavlovian conditioning. We predicted that IL-to-NAcS stimulation would suppress conditioned responding by facilitating the retrieval of a previously established extinction memory.

Materials and Methods

Subjects. One hundred male Long-Evans rats (220–240 g on arrival; Charles River Laboratories) were pair housed on arrival and single housed 3 d later. Rats were housed in polycarbonate home cages (44.5 cm × 25.8 cm × 21.7 cm) containing sani-chip bedding (catalog #7090A, Envigo), a nylon bone toy, (catalog #K3580, Bio-Serv), and a tunnel (catalog #K3245, Bio-Serv). Rats had access to food (catalog #5075, Charles River Laboratories) and water *ad libitum* in their home cages throughout the experiment. Home cages were in a colony room with controlled temperature (21°C) and humidity (44%) on a 12 h light/dark cycle (lights on at 7:00 A.M.). All procedures were conducted during the light phase. All procedures were approved by the Animal Research Ethics Committee of Concordia University and in accordance with the guidelines from the Canadian Council on Animal Care.

Apparatus. Behavioral procedures were conducted in six conditioning chambers (catalog #ENV-009A, Med Associates), housed in sound-attenuating melamine cubicles. Chambers contained bar floors, a house light (75 W, 100 mA; catalog #ENV-215M, Med Associates) in the center of the left wall, and a white-noise generator and speaker (5 dB above background noise; catalog #ENV-225SM, Med Associates) in the top left corner of the left wall. A customized fluid port (opening height of 13.2 cm; catalog #ENV-200R3AM, Med Associates) was used to ease port access and was located 2 cm above the bar floor in the center of the right wall. Infrared sensors (catalog #ENV-254CB, Med Associates) flanked both sides of the port opening to detect port entries. Solutions were delivered into the fluid port via a polyethylene tube (catalog #141691A, Fisher Scientific) connected to a 20 ml syringe in a pump (model #PHM-100, 3.33 rpm) located outside the cubicle. All events, peripheral devices, and data collection were controlled by Med Associates software (Med-PC IV) on a computer.

Optogenetic stimulation was delivered in each conditioning chamber by a 150 mW, 473 nm laser (catalog #BL473T3-150, Shanghai Laser & Optics Century). The laser was connected to a unilateral optical rotary joint (catalog #FRJ-FC-FC, Doric Lenses) via a 125 μm optical fiber (catalog #FC-FCFC-MS6-2M, Fiber Optic Cable Shop). A custom-made patch cord (Trujillo-Pisanty et al., 2015) containing a 200 μm fiber connected the rotary joint to a custom-made optical fiber implant containing a 300 μm fiber. Before each test, the power of the laser was calibrated to ~30 mW for each optical fiber implant. Optogenetic stimulation was delivered at a frequency of 20 Hz (5 ms pulses) in a 10.2 s pulse train programmed through an Arduino Tech microcontroller. Optogenetic parameters were based on our previous study (Villaruel et al., 2018) and other studies (Adamantidis et al., 2011; Britt et al., 2012).

Solutions and viruses. A 10% (w/v) sucrose solution was prepared by mixing sucrose (catalog #SUC600, Bioshop) in tap water and served as the unconditioned stimulus. Odors used in experiment 1 were prepared by diluting lemon oil (catalog #W262528-1KG-K, Sigma-Aldrich) or benzaldehyde (Almond Odour, catalog #B1000, ACP Chemicals) with water to make a 10% solution. Viruses containing the transgene for channelrhodopsin-2 (ChR2) with the enhanced yellow fluorescent protein (eYFP) reporter (AAV5-CaMKIIa-hChR2(H134R)-EYFP, 1.5×10^{13} Vg/ml; Addgene) or eYFP alone (AAV2-CaMKIIa-EYFP, 2.0×10^{12} Vg/ml; Addgene; AAV5-CaMKIIa-EYFP, 9.0×10^{12} Vg/ml, Neurophotonics) were used for optogenetic surgeries.

Surgery. Rats received stereotaxic surgery using standard procedures starting 1 week after single housing. Target coordinates for the IL were + 2.9 mm anterior and + 3.4 mm lateral compared to bregma and −5.8 mm ventral compared to the skull surface (30° angle). The viral vector containing the transgene for ChR2 or eYFP alone was microinfused into the IL (1 μl, 0.1 μl/min, 20 min diffusion). Microinfusion was conducted through a blunted 27 gauge needle (catalog #14-821-13B, Fisher Scientific) connected via polyethylene tubing (PE20, catalog #CA-63018-645, VWR) to a 10 μl Hamilton syringe (model #1701 N, Hamilton) on a pump (Pump 11 Elite, catalog #70-4501, Harvard Apparatus). An optical fiber implant was inserted into the NAcS

[anteroposterior (AP) + 1.2 mm, mediolateral (ML) + 1.0 mm, from bregma and dorsoventral (DV) −7.5 mm from the skull surface] or BLA (AP −2.5 mm, ML −5.0 mm, from bregma and DV −8.5 mm from the skull surface) in the same hemisphere. Optical fiber implants were secured using five jeweler's screws, Metabond (catalog #553-3484, Patterson Dental), and dental acrylic (powder, catalog #525000, solvent, catalog #526000, A-M Systems). Buprenorphine (Buprenex, 0.03 mg/kg, s.c.) was administered as an analgesic after surgery. To facilitate recovery, rats were provided with banana-flavored oral rehydrator (PRANG, catalog #F2351-B, Bio-Serv) for 48 h after surgery. Behavioral tests involving optogenetic stimulation were done at least 8 weeks after surgery to ensure ample time for virus expression.

Retrograde tracing with Cholera toxin subunit B (CTb, catalog #C34775 and #C34776, Thermo Fisher Scientific) was used to characterize the IL-to-NAcS and IL-to-BLA neural circuits. Rats (n = 4) underwent stereotaxic surgery in which CTb conjugated with either Alexa Fluor 488 or Alexa Fluor 555 (0.5% weight/volume in 0.9% sterile saline) was unilaterally infused into the NAcS or BLA (0.3 μl, 0.1 μl/min, 10 min diffusion). Coordinates from bregma (AP and ML) and the skull surface (DV) for targeting the NAcS were AP + 1.2 mm, ML + 1.0 mm, DV −7.5 mm, and for the BLA were AP −2.5 mm, ML −5.0 mm, DV −8.5 mm. The fluorescent label used for tracing was counterbalanced by region across rats.

General behavioral procedures. Rats were handled and weighed before each procedure. Rats were exposed to 10% sucrose through a bottle in their home cage in two 24 h sessions to acclimate them to the taste of sucrose. Rats were habituated to the conditioning chambers in 20 min sessions in which the house light was on, and port entries were recorded. After the last habituation, rats received daily Pavlovian conditioning sessions (40 min). At 2 min after initiating the program, the house light was illuminated to signal the start of the session. Sessions consisted of 14 presentations of a 10 s continuous white-noise CS occurring at a variable-time 140 s schedule [intertrial intervals (ITIs) 80, 140, or 200 s]. Pumps were activated 4 s after CS onset to deliver 0.2 ml of sucrose into the fluid port (2.8 ml per session) and coterminated with the CS. Ports were checked after each session to ensure sucrose consumption. Extinction sessions and tests occurred just as Pavlovian conditioning but without sucrose. In all sessions, rats were tethered to a patch cord. However, patch cords were only functional during test sessions.

Experiment 1: Effect of IL-to-NAcS stimulation on context-induced renewal of appetitive Pavlovian conditioned responding. Experiment 1 tested whether optogenetic stimulation of the IL-to-NAcS circuit during CS trials would attenuate context-induced renewal of appetitive Pavlovian conditioned responses after extinction. Rats were habituated in conditioning chambers of a default configuration consisting of clear walls, bar floors, and no odors. Conditioning and extinction sessions occurred in distinct contexts as previously described (Villaruel et al., 2018). The conditioning context was referred to as Context A, and the extinction context as Context B. The configuration of Contexts A and B was counterbalanced between two types. Context type 1 consisted of bar floors, black-and-white striped walls, and a lemon odor. Context type 2 consisted of wire grid floors, clear walls, and an almond odor. Odors were applied to Petri dishes located underneath the floor of the conditioning chambers.

Groups consisted of rats microinfused with ChR2 (n = 10) or eYFP alone (n = 10). Rats received five successive habituation sessions for the following: transport, the experimental room, being tethered to a patch cord in a default conditioning chamber, and the conditioning and extinction contexts. The order of habituation in the conditioning and extinction contexts was counterbalanced across rats. Habituation in the conditioning context involved fluid port training consisting of five unsignaled deliveries of sucrose with an interdelivery interval of 240 s. After habituation, rats received 12 Pavlovian conditioning sessions in Context A, followed by at least three extinction sessions in Context B or until a criterion of five or fewer CS port entries was met. Following extinction, rats were tested in Contexts A and B across 2 d. Test order was counterbalanced so that half of the rats were tested in Context A first and the other half in Context B first. Test sessions were separated by at least one extinction session or until the criterion of five or fewer CS port entries was met to mitigate any after effects of optogenetic stimulation. We found that rats in the eYFP group that received their second test in Context A did not show renewal. Therefore, after test 2, all rats received two Pavlovian reconditioning sessions in Context A and at least two extinctions in Context B or until the criterion was met before repeating the second renewal test. Final data analysis consists of collapsing the first renewal test and the repeated second test.

A supplementary experiment tested whether optogenetic stimulation of the IL-to-BLA circuit would attenuate context-induced renewal of appetitive Pavlovian conditioning because of its proposed role in extinction of aversive Pavlovian conditioned responding (Peters et al., 2009; Bloodgood et al., 2018). This experiment consisted of rats all microinfused with ChR2 (n = 6). Habituation and context configurations were identical to the IL-to-NAcS renewal experiment. After habituation, rats received 10 Pavlovian conditioning sessions in Context A and at least three extinction sessions in Context B or until the criterion of five or fewer CS port entries was met. One day after the last extinction session, rats were tested for renewal in Context A with optogenetic stimulation occurring either during the CS or in the middle of the ITIs. Test order was counterbalanced so that half of the rats were tested with optogenetic stimulation occurring during the CS first and for the other half during the ITI first. Optogenetic stimulation of the IL during the ITI does not affect renewal, and therefore this group served as a within-subject control (Villaruel et al., 2018). Between tests, rats received three Pavlovian conditioning sessions in Context A followed by at least two extinction sessions or until criterion was met.

Experiment 2: Effect of IL-to-NAcS stimulation on the suppression of appetitive Pavlovian conditioned responding after extinction. Experiment 2 tested whether prior extinction training was necessary for IL-to-NAcS stimulation to suppress appetitive Pavlovian conditioned responding. Rats were habituated to the following: transport, the experimental room, and the conditioning chamber while tethered to a patch cord. All behavioral sessions occurred in default conditioning chambers devoid of additional contextual cues. Rats then received 10 daily sessions of Pavlovian conditioning. Next, rats microinfused with ChR2 (n = 26) or eYFP alone (n = 22) were divided into either an Extinction group or No Extinction group matched on the acquisition of Pavlovian conditioning and CS port entries in the last conditioning session. Rats in the Extinction group (ChR2, n = 13; eYFP, n = 11) received one extinction session 24 h after the last conditioning session. In contrast, rats in the No Extinction group (ChR2, n = 13; eYFP n = 11) did not receive extinction training and were instead handled and weighed in the colony room. The following day, all rats underwent a reconditioning session to re-establish baseline responding. An extinction test (test 1) was conducted the following day and was identical to an extinction session but with optogenetic stimulation delivered during CS trials. An extinction retrieval test (test 2) was conducted the next day and was identical to an extinction session but occurred without the delivery of optogenetic stimulation.

Experiment 3: Effect of IL-to-NAcS circuit stimulation on the acquisition and expression of appetitive Pavlovian conditioning. Experiment 3 tested whether IL-to-NAcS stimulation would indiscriminately suppress CS responding, thereby preventing the acquisition of appetitive Pavlovian conditioning. Rats (ChR2, n = 11; eYFP, n = 11) were habituated to transport, the experimental room, and the conditioning chamber while tethered to a patch cord. All behavioral sessions occurred in default conditioning chambers. Rats received 12 daily sessions of Pavlovian conditioning as previously described, except that optogenetic stimulation was delivered during CS trials.

Following conditioning, we examined the effect of IL-to-NAcS stimulation on the expression of conditioned responding. Rats were tested across two sessions approximately 24 h apart for the expression of conditioned responding to the CS alone in the absence of the sucrose US. In one test optogenetic stimulation during the CS was present, and in the other test optogenetic stimulation was withheld. Test order was counterbalanced across rats, and rats were matched based on acquisition of Pavlovian conditioning measured by Δ CS port entries.

Histology. All rats were killed with a pentobarbital (Euthanyl) overdose and transcardially perfused with 0.1 M PBS followed by 4% paraformaldehyde (PFA) in 0.1 M phosphate buffer. Brains were extracted and postfixed in 4% PFA solution for 24 h, followed by a 30% sucrose solution for 48 h in 4°C. Brains were frozen at −80°C and sectioned using a cryostat (40 μm) in a one-in-five series. Brain sections were mounted onto microscope slides and processed for Nissl staining or fluorescence microscopy with DAPI (catalog #H-1200, Vector Laboratories) to verify optical fiber placement and transgene expression. Images of transgene expression were captured through an epifluorescence microscope (Nikon Eclipse TiE) using a 4× lens for cell bodies and a 20× lens for neuron terminals. A rat brain atlas (Paxinos and Watson, 2007) was used to approximate the location of sections compared to bregma, and the images were used to model the spread of transgene expression in the IL (Adobe Illustrator).

Rats in the retrograde tracing experiment were killed 1 week after receiving surgery, and brains were processed as described above. Brain sections were stained with DAPI, coverslipped, and processed through fluorescence microscopy. Infusion sites were examined to ensure accurate targeting of the NAcS and the BLA using an epifluorescence microscope with a 4× lens. A confocal laser scanning microscope (Nikon C2) was used to image CTb-labeled cells in the medial prefrontal cortex (four sections per rat) using a 20× lens. Images were imported to Imaris Cell Imaging Software (Bitplane, Oxford Instruments) in which analysis was specifically restricted to the IL by the experimenter using a rat brain atlas (Paxinos and Watson, 2007). CTb-488- and CTb-555-labeled cells were defined using the blobs tool in Imaris, local contrast thresholding, and volume of labeled pixels. Colabeling of CTb-488 and CTb-555 signals was determined as objects labeled in one channel that had >20% of their volume also labeled in the second channel. The number of labeled and colabeled cells was averaged across the four sections to get a single value for each rat. Density of labeled and colabeled cells was calculated by dividing the average number of labeled and colabeled by the average area of the selected quantified region across four brain sections.

Fos immunohistochemistry. Rats in experiment 1 received an additional test to induce Fos and verify that optogenetic stimulation of IL-to-NAcS and IL-to-BLA terminals expressing ChR2 had a physiological effect (Fuchikami et al., 2015; Benn et al., 2016; Wood et al., 2019). The Fos induction session occurred in default conditioning chambers and was identical to that of previous test sessions. Optogenetic stimulation was delivered for 14 trials to mimic previous tests but in the absence of house light illumination, the white-noise CS, or sucrose. In the IL-to-BLA experiment, optogenetic stimulation was omitted in half of the rats to include a nonstimulated control. Rats remained in the conditioning chambers for an additional 50 min to ensure that they were killed 90 min after the start of the session to maximize Fos expression (Müller et al., 1984; Bossert et al., 2011; Warren et al., 2016). Brain sections were processed in an anti-*cfos* rabbit antibody (1:2000; catalog #2250S, Cell Signaling Technology) for ~72 h and subsequently in a secondary solution with biotinylated goat anti-rabbit antibody (1:250; catalog #BA-1000, Vector Laboratories). Next, sections were placed in a tertiary of avidin and biotinylated horseradish peroxidase (1:1000; ABC kit, catalog #PK-6100, Vector Laboratories) and stained with a 3, 3′-diaminobenzidine solution. Finally, sections were rinsed in phosphate buffer, mounted on slides, and coverslipped. Images of each section were captured through a brightfield microscope (Nikon Eclipse TiE) using a 10× lens. Two sections from the IL, the NAcS, or the BLA were chosen for quantification based on location compared to bregma and image quality. A rat brain atlas (Paxinos and Watson, 2007) was used to approximate the location of sections compared to bregma and the regions of interest. Image analysis was done through ImageJ Fiji. A region of the IL, the NAcS, and BLA was selected manually for each section in both the stimulated and nonstimulated hemisphere. Quantification of the selection was done through a custom-made Fiji macro, which counted Fos-positive nuclei based on color compared to background, size, and circularity. Counts were then divided by the average area selected in Fiji to calculate density. The final Fos density for each rat consisted of the average across two sections for each hemisphere and region.

Statistical tests. Data were processed in Microsoft Excel, visualized in Prism (GraphPad), and analyzed in SPSS (IBM). Behavioral data of interest included port entries made during the entire session (total), 10 s before CS onset (Pre CS), during the 10 s CS (CS), 10 s after CS onset (Post CS), and during the intertrial intervals (between Post CS offset and Pre CS onset). Conditioned responding was measured using a difference score (Δ CS Port Entries) calculated by subtracting port entries made during the Pre CS period from the CS period to account for variability in baseline activity (Rhodes and Killcross, 2004, 2007; Villaruel et al., 2018). Δ CS port entries were also analyzed across CS trials. Probability, duration, and latency of CS port entries were collected and analyzed both as an average in the session and per CS trial. Probability was calculated as the number of trials with a port entry divided by the total number of trials (14). Duration was measured as time in the port after initiating a port entry during the CS. Latency was measured as time to initiate the first CS port entry. Data were analyzed using ANOVA, and all significant interactions were further examined with Bonferroni-corrected comparisons. The α level for statistical significance was set to 0.05.

Results

Histology

We used a retrograde tracer (Cholera toxin B) to characterize neural projections from the IL-to-NAcS and IL-to-BLA (Fig. 1*A–D*). Neural tracing of IL projections to the NAcS and BLA revealed largely distinct, nonoverlapping projections to these output regions. Only a small proportion of labeled cells was found to project to both the NAcS and the BLA (Fig. 1*D*; $F_{(2,11)} = 33.21$, $p < 0.001$). Density of labeled cells in the NAcS ($p < 0.001$) and BLA ($p = 0.001$) were greater than from both output regions. Density of labeled cells were similar between the NAcS and BLA ($p = 0.154$).

Figure 1*E* depicts the expression of the ChR2 transgene observed in the IL. The approximate spread of the transgenes for ChR2 and eYFP alone was based on rats in experiment 1 but was consistent across experiments (Fig. 1*F*). The highest concentration of ChR2 expression was in the infralimbic cortex, the dorsal peduncular cortex, and the ventral regions of the prelimbic cortex. Some expression of ChR2 was observed along the injector tract, in the anterior and lateral areas of the prelimbic cortex along the forceps minor of the corpus callosum, and the anterior medial and ventral orbitofrontal cortex.

In all experiments, rats were excluded from final behavioral data analysis because of lack of transgene expression or misplacement of optical fiber implants. In experiment 1, two rats (eYFP, $n = 1$; ChR2, $n = 1$) were excluded because of misplaced optical fiber implants. The final group sizes for experiment 1 were ChR2, $n = 9$, and eYFP, $n = 9$. One additional rat (eYFP, $n = 1$) from experiment 1 was removed from Fos immunohistochemistry analysis because of complications with histology. The final group size for the IL-to-BLA experiment was ChR2, $n = 6$. In experiment 2, two rats (eYFP, $n = 1$; ChR, $n = 1$) were excluded because of misplaced optical fiber implants, and one rat (eYFP, $n = 1$) was excluded because of lack of transgene expression. The final group sizes for experiment 2 were ChR2 Extinction, $n = 13$; ChR2 No Extinction, $n = 12$; eYFP Extinction, $n = 10$; and eYFP No Extinction, $n = 10$. The final group sizes for experiment 3 were ChR2, $n = 11$, and eYFP, $n = 11$.

IL-to-NAcS stimulation induced Fos reactivity in the IL and NAcS

Fos immunohistochemistry was conducted on a subset of rats from experiment 1 (ChR2, $n = 9$; eYFP, $n = 8$) to verify that optogenetic stimulation of the IL-to-NAcS circuit activated the IL and the NAcS (Fig. 2*A*). In the IL (Fig. 2*B*, left), Fos

immunoreactivity was greater in rats expressing ChR2 than eYFP alone (Fig. 2*C*, left; Virus, $F_{(1,15)} = 40.70$, $p < 0.001$) and in the stimulated hemisphere compared to the noninfected, nonstimulated, control hemisphere (Hemisphere, $F_{(1,15)} = 9.50$, $p = 0.008$). Density of Fos-positive nuclei in the IL showed a statistically significant interaction between virus and hemisphere (Hemisphere × Virus, $F_{(1,15)} = 9.68$, $p = 0.007$). The stimulated hemisphere had greater Fos immunoreactivity than the nonstimulated hemisphere in the ChR2 group ($p < 0.001$) but not in the eYFP group ($p = 0.984$).

The ChR2 group had greater Fos density than the eYFP group in both the stimulated hemisphere ($p < 0.001$) and the nonstimulated hemisphere ($p = 0.011$). These results indicate that optogenetic stimulation of IL neuron terminals in the NAcS activated the IL. However, optogenetic stimulation of the ChR2-transfected hemisphere also activated the opposite, nonstimulated hemisphere.

In the NAcS (Fig. 2*B*, right), Fos immunoreactivity was greater in rats expressing ChR2 than eYFP alone (Fig. 2*C*, right; Virus, $F_{(1,15)} = 20.26$, $p < 0.001$) and in the stimulated hemisphere compared to the nonstimulated hemisphere (Hemisphere, $F_{(1,15)} = 27.39$, $p < 0.001$). A statistically significant interaction was observed in Fos density in the NAcS (Hemisphere × Virus, $F_{(1,15)} = 17.60$, $p = 0.001$). Greater Fos immunoreactivity was observed in the stimulated hemisphere compared to the nonstimulated hemisphere in the ChR2 group ($p < 0.001$) but not in the eYFP group ($p = 0.486$). Fos density in the ChR2 group was also greater than in the eYFP group in both the stimulated ($p < 0.001$) and nonstimulated hemisphere ($p = 0.026$). Therefore, optogenetic stimulation of IL neuron terminals in the NAcS activated the NAcS. As with the IL, optogenetic stimulation of the ChR2-transfected hemisphere also induced moderate activation in the nonstimulated hemisphere in the NAcS.

In a separate set of rats (ChR2, $n = 6$), Fos immunohistochemistry was conducted to verify that optogenetic stimulation of the IL-to-BLA circuit activated the IL and the BLA (Fig. 3*A*). Density of Fos-positive nuclei in the IL (Fig. 3*B*, left) showed a statistically significant interaction between laser stimulation and hemisphere (Fig. 3*C*, left; Hemisphere, $F_{(1,4)} = 20.38$, $p = 0.011$; Stimulation, $F_{(1,4)} = 5.00$, $p = 0.089$; Hemisphere × Stimulation, $F_{(1,4)} = 34.09$, $p = 0.004$). Rats that received laser stimulation (Laser ON) had greater Fos immunoreactivity than rats that did not receive laser stimulation (Laser OFF) in the stimulated hemisphere containing the optical fiber ($p = 0.021$) but not the nonstimulated hemisphere ($p = 0.708$). The stimulated hemisphere containing the optical fiber had greater Fos immunoreactivity than the nonstimulated hemisphere in rats that received laser stimulation ($p = 0.002$) but not in rats that did not receive laser stimulation ($p = 0.402$). In the BLA (Fig. 3*B*, right), density of Fos-positive nuclei was greater in rats that received laser stimulation compared to rats that did not receive laser stimulation regardless of hemisphere (Fig. 3*C*, right; Hemisphere, $F_{(1,4)} = 0.96$, $p = 0.384$; Stimulation, $F_{(1,4)} = 8.73$, $p = 0.042$; Hemisphere × Stimulation, $F_{(1,4)} = 3.88$, $p = 0.120$). Together, these results indicate that optogenetic stimulation of IL terminals in the BLA activated the IL and BLA.

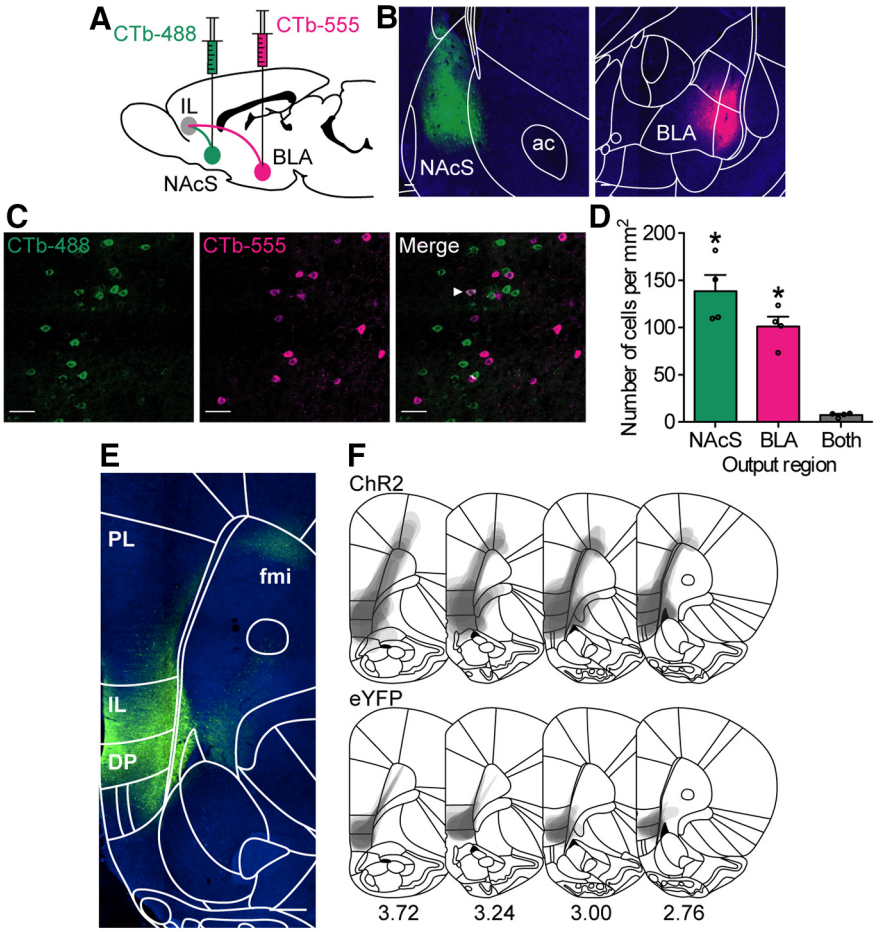

Figure 1. Neural tracing and optogenetic targeting of IL neural circuits. ***A***, Method schematic for neural tracing. CTb-488 and CTb-555 retrograde tracers were injected in the NAcS and the BLA, and quantification of labeled cells was done in the IL. ***B***, Representative images of injection sites in the NAcS (left) and the BLA (right). ac, Anterior commissure. Scale bar, 100 μm. ***C***, Representative images of labeled cells in the IL. Arrow in merged image shows an example of colabeling. Scale bar, 50 μm. ***D***, Quantification of labeled cells in the IL shows largely nonoverlapping cells projecting to the NAcS and the BLA. Data indicate mean ± SEM; *$p < 0.05$, output region versus Both output regions. ***E***, Representative image of ChR2 expression in the IL. PL, Prelimbic cortex; DP, Dorsal peduncular cortex; fmi, forceps minor of the corpus callosum. Scale bar, 500 μm. ***F***, Schematic depicting the extent of ChR2 ($n = 9$, top) and eYFP alone ($n = 9$, bottom) expression in the IL across four bregma points.

IL-to-NAcS stimulation suppressed context-induced renewal of appetitive Pavlovian conditioned responding

Experiment 1 tested whether optogenetic stimulation of the IL-to-NAcS circuit would suppress the renewal of appetitive Pavlovian conditioned responding after extinction. Both ChR2 and eYFP groups similarly acquired Pavlovian conditioning in Context A as measured by Δ CS port entries (Fig. 4*E*, Session, $F_{(11,176)} = 14.59$, $p < 0.001$; Virus, $F_{(1,16)} = 0.17$, $p = 0.684$; Session × Virus, $F_{(11,176)} = 0.62$, $p = 0.679$) and extinguished

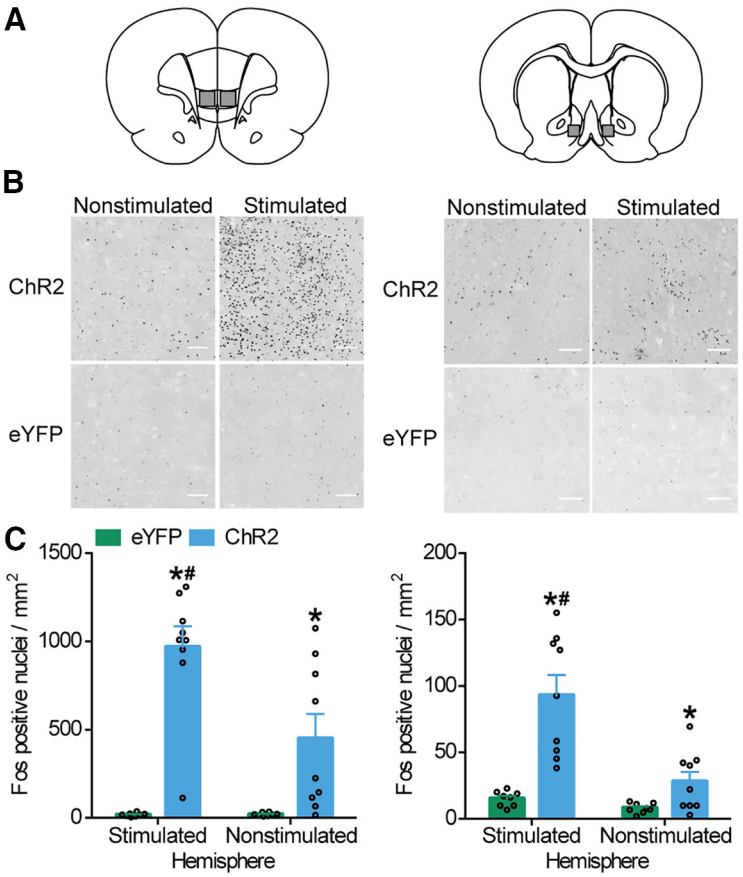

Figure 2. Quantification of Fos-positive nuclei density following optogenetic stimulation of the IL-to-NAcS circuit. ***A***, Schematic depicting demarcations in the images of the IL (left) and NAcS (right) quantified for Fos-positive nuclei. ***B***, Representative images of Fos-positive nuclei in the IL (left) and NAcS (right) in the Stimulated and Nonstimulated hemisphere of rats expressing ChR2 or eYFP alone. Scale bars: 100 μm. ***C***, Density of Fos-positive nuclei (mean ± SEM) in the IL (left) and the NAcS (right) in rats expressing ChR2 or eYFP alone in both the Stimulated hemisphere containing the optical fiber and in the Nonstimulated hemisphere without an optical fiber; *$p < 0.05$, ChR2 versus eYFP in each hemisphere; #$p < 0.05$, Stimulated versus Nonstimulated hemisphere in the ChR2 group.

conditioned responding in the first three sessions of extinction in Context B (Session, $F_{(2,32)} = 16.84$, $p < 0.001$; Virus, $F_{(1,16)} = 2.08$, $p = 0.168$; Session × Virus, $F_{(2,32)} = 1.41$, $p = 0.259$). Virus groups did not differ in the last session of extinction before tests (Virus, $F_{(1,16)} = 0.51$, $p = 0.487$). Both ChR2 and eYFP groups similarly reacquired (Fig. 4*F*; Session, $F_{(1,16)} = 0.004$, $p = 0.949$; Virus, $F_{(1,16)} = 1.06$, $p = 0.319$; Session × Virus, $F_{(1,16)} = 0.02$, $p = 0.898$) and re-extinguished (Session, $F_{(1,16)} = 13.67$, $p = 0.002$; Virus, $F_{(1,16)} = 3.16$, $p = 0.094$; Session × Virus, $F_{(1,16)} = 0.04$, $p = 0.854$) conditioned responding following the first round of testing. Groups did not differ in Δ CS port entries in the last session of extinction before the second round of tests (Virus, $F_{(1,16)} = 0.53$, $p = 0.476$).

Optogenetic stimulation of the IL-to-NAcS during CS trials in the ChR2 group suppressed context-induced renewal of appetitive Pavlovian conditioned responding (Fig. 4*G*). In the renewal tests, the eYFP but not the ChR2 group showed a robust renewal of conditioned responding in Context A compared to Context B (Context, $F_{(1,16)} = 18.38$, $p = 0.001$; Virus, $F_{(1,16)} = 4.96$, $p = 0.041$; Context × Virus, $F(1,16) = 51.04$, $p < 0.001$). Δ CS port entries were low for both eYFP and ChR2 at test in the extinction Context B ($p = 0.644$). However, Δ CS port entries were greater in the eYFP group compared to the ChR2 group in Context A ($p < 0.001$), indicating that stimulation of the IL-to-NAcS during CS trials suppressed renewal. The eYFP group showed greater Δ CS port entries at test in Context A compared to Context B ($p < 0.001$). In contrast, the ChR2 group showed similar levels of low responding in both Contexts A and B ($p = 0.060$).

Analysis of Δ CS port entries across trials at test showed that IL-to-NAcS stimulation during CS trials suppressed conditioned responding in all trials (Figure 4*H*; Context, $F_{(1,16)} = 18.38$, $p = 0.001$; Virus, $F_{(1,16)} = 4.96$, $p = 0.041$; Context × Virus, $F_{(1,16)} = 51.04$, $p < 0.001$; Trial, $F_{(13,208)} = 1.37$, $p = 0.208$; Trial × Virus, $F_{(13,208)} = 1.49$, $p = 0.162$; Context × Trial, $F_{(13,208)} = 0.68$, $p = 0.680$; Context × Trial × Virus, $F_{(13,208)} = 0.83$, $p = 0.558$). Δ CS port entries were similar for ChR2 and eYFP groups in Context B ($p = 0.644$). However, at test in Context A, the eYFP group had greater CS port entries compared to the ChR2 group ($p < 0.001$). The eYFP group exhibited renewal and showed greater Δ CS responding in Context A compared to Context B ($p < 0.001$). In contrast, the ChR2 group had equivalent responding across all trials in Contexts A and B ($p = 0.060$). These results suggest that optogenetic stimulation of the IL-to-NAcS circuit suppressed appetitive Pavlovian conditioned responding throughout the renewal test.

Stimulation of the IL-to-NAcS neural circuit did not affect port entries made during the ITIs (Fig. 4*I*). Port entries made during the ITIs were greater in Context A than in Context B in both ChR2 and eYFP groups (Context, $F_{(1,16)} = 6.24$, $p = 0.024$; Virus, $F_{(1,16)} = 1.05$, $p = 0.322$; Context × Virus, $F_{(1,16)} < 0.01$, $p = 0.986$). Therefore, optogenetic stimulation of the IL-to-NAcS circuit did not produce nonspecific motor effects during time intervals outside the CS and stimulation.

Additional measures of conditioned responding further support that optogenetic stimulation of the IL-to-NAcS during CS trials suppressed context-induced renewal of appetitive Pavlovian conditioned responding (Fig. 4*J–L*). In the renewal tests, the eYFP but not the ChR2 group displayed robust renewal in Context A compared to Context B as measured by probability of CS port entries (Fig. 4*J*; Context, $F_{(1,16)} = 21.647$, $p < 0.001$; Virus, $F_{(1,16)} = 4.09$, $p = 0.060$; Context × Virus, $F_{(1,16)} = 19.34$, $p < 0.001$), total duration of port entries initiated during the CS (Fig. 4*K*; Context, $F_{(1,16)} = 20.12$, $p < 0.001$; Virus, $F_{(1,16)} = 12.57$, $p = 0.003$; Context × Virus, $F_{(1,16)} = 15.26$, $p = 0.001$), and average latency to initiate a CS port entry (Fig. 4*L*; Context, $F_{(1,16)} = 19.73$, $p < 0.001$; Virus, $F_{(1,16)} = 3.75$, $p = 0.071$; Context × Virus, $F_{(1,16)} = 14.16$, $p = 0.002$). Probability ($p = 0.918$), duration ($p = 0.293$), and latency ($p = 0.959$) were similar for both eYFP and ChR2 groups at test in the extinction Context B. However, probability ($p = 0.006$) and duration ($p = 0.001$) were higher, and latency was shorter ($p = 0.010$) in the eYFP group compared with the ChR2 group in Context A, indicating that stimulation of the IL-to-NAcS during CS trials suppressed renewal. The eYFP group showed greater probability ($p < 0.001$) and duration ($p < 0.001$) and shorter latency ($p < 0.001$) of CS port entries at test in Context A compared

to Context B. In contrast, the ChR2 group showed similar levels of probability (p = 0.860), duration (p = 0.688), and latency (p = 0.638) at tests in both Context A and B.

Altogether, optogenetic stimulation of the IL-to-NAcS neural circuit during CS trials attenuated the renewal of appetitive Pavlovian conditioned responding and did not affect port entries outside of the CS.

In a separate group of rats (n = 6), we tested whether optogenetic stimulation of the IL-to-BLA neural circuit would affect renewal of appetitive Pavlovian conditioned responding (Fig. 5). Δ CS port entries increased during conditioning in Context A (Fig. 5*E*; Session, $F_{(9,45)}$ = 9.08, $p < 0.001$), was lower during extinction in Context B (Session, $F_{(2,10)}$ = 1.58, p = 0.254), and remained low in the last extinction session before the first renewal test. Δ CS port entries remained high across three reconditioning sessions (Fig. 5*F*; Session, $F_{(2,10)}$ = 1.14, p = 0.359), was lower during the re-extinction sessions (Session, $F_{(1,5)}$ = 0.54, p = 0.494), and was maintained at low levels in the last extinction session before the second renewal test.

Optogenetic stimulation of the IL-to-BLA circuit during CS trials did not affect context-induced renewal of appetitive Pavlovian conditioned responding (Fig. 5*G*). Rats exhibited renewal with greater Δ CS port entries at test compared to the last extinction session regardless of whether optogenetic stimulation of the IL-to-BLA circuit occurred during the CS or in the ITI (Phase, $F_{(1,5)}$ = 10.94, p = 0.021; Stimulation, $F_{(1,5)}$ = 0.81, p = 0.409; Phase × Stimulation, $F_{(1,5)}$ = 0.114, p = 0.749). Δ CS port entries across trials during the renewal tests were similar regardless of whether IL-to-BLA circuit stimulation occurred during the CS or the ITI (Fig. 5*H*; Stimulation, $F_{(1,5)}$ = 0.38 p = 0.563; Trial, $F_{(13,65)}$ = 1.49, p = 0.224; Stimulation × Trial, $F_{(13,65)}$ = 0.68, p = 0.762). Port entries during the ITI were also similar across extinction and renewal regardless of the time of IL-to-BLA stimulation (Fig. 5*I*; Phase, $F_{(1,5)}$ = 1.02, p = 0.359; Stimulation, $F_{(1,5)}$ = 2.94, p = 0.147; Phase × Stimulation, $F_{(1,5)}$ = 0.110, p = 0.754).

Additional measures of conditioned responding further support that IL-to-BLA stimulation did not affect context-induced renewal of appetitive Pavlovian conditioned responding. Probability (Fig. 5*J*; Phase, $F_{(1,5)}$ = 29.48, p = 0.003; Stimulation, $F_{(1,5)}$ = 0.44, p = 0.538; Phase × Stimulation, $F_{(1,5)}$ = 0.27, p = 0.627) and duration (Fig. 5*K*; Phase, $F_{(1,5)}$ = 46.72, p = 0.001; Stimulation, $F_{(1,5)}$ = 0.01, p = 0.948; Phase × Stimulation, $F_{(1,5)}$ = 0.003, p = 0.962) of CS port entries were greater in the renewal test compared with the last extinction session regardless of whether IL-to-BLA stimulation occurred during the CS or the ITI at test. Finally, latency to initiate a CS port entry decreased from the last session of extinction compared to the renewal test and was not affected by IL-to-BLA stimulation during the CS or the ITI (Fig. 5*L*; Phase, $F_{(1,5)}$ = 30.35, p = 0.003; Stimulation, $F_{(1,5)}$ = 0.08, p = 0.786; Phase × Stimulation, $F_{(1,5)}$ = 0.25, p = 0.642).

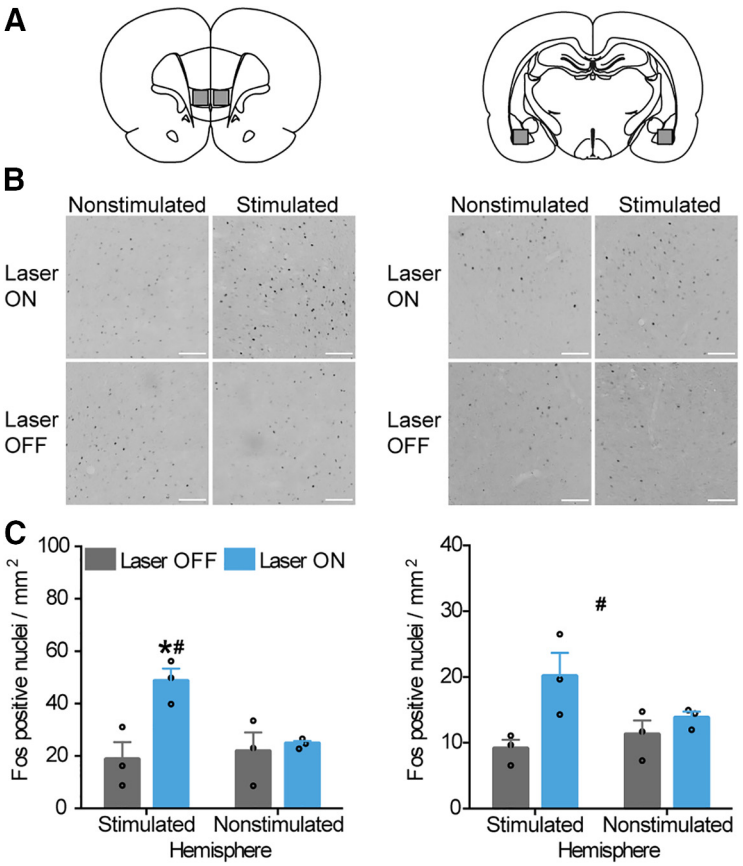

Figure 3. Quantification of Fos-positive nuclei density following optogenetic stimulation of the IL-to-BLA circuit. ***A***, Schematic depicting demarcations in the images of the IL (left) and BLA (right) quantified for Fos-positive nuclei. ***B***, Representative images of Fos-positive nuclei in the IL (left) and BLA (right) in the Stimulated and Nonstimulated hemisphere of ChR2-expressing rats that received laser stimulation (Laser ON) or no laser stimulation (Laser OFF). Scale bars, 100 μm. ***C***, Density of Fos-positive nuclei (mean ± SEM) in the IL (left) and the BLA (right) in rats that received laser stimulation or no laser stimulation in both the Stimulated hemisphere containing the optical fiber and in the Nonstimulated hemisphere without an optical fiber. Left graph, *$p < 0.05$, laser ON versus laser OFF in the Stimulated hemisphere; #$p < 0.05$ Stimulated versus Nonstimulated hemisphere in the laser ON group. Right graph, #$p < 0.05$ main effect of laser stimulation.

Altogether, optogenetic stimulation of the IL-to-BLA neural circuit during CS trials did not affect the renewal of appetitive Pavlovian conditioned responding.

IL-to-NAcS stimulation suppressed appetitive Pavlovian conditioned responding regardless of prior extinction

Experiment 2 tested whether prior extinction training and the establishment of an inhibitory extinction memory were necessary for optogenetic stimulation of the IL-to-NAcS to suppress appetitive Pavlovian conditioned responding. All groups displayed an equivalent increase in Δ CS port entries across Pavlovian conditioning sessions (Fig. 6*C*; Session, $F_{(4,161)}$ = 41.52, p = 0.001) with no effect of virus (Virus, $F_{(1,41)}$ = 1.90, p = 0.176) or extinction group (Group, $F_{(1,41)}$ = 0.14, p = 0.708) and no statistically significant interactions (Session × Virus, $F_{(9,369)}$ = 1.17, p = 0.326; Session × Group, $F_{(9,369)}$ = 0.48, p = 0.780; Virus × Group, $F_{(1,41)}$ = 0.03, p = 0.872; Session × Virus × Group, $F_{(9,369)}$ = 1.06, p = 0.380). Δ CS port entries were equal between ChR2 Extinction and eYFP Extinction groups during the extinction session (Virus, $F_{(1,21)}$ = 0.19, p = 0.670). The ChR2 Extinction and eYFP Extinction groups had similar within-session reduction of Δ CS port entries across trials during the extinction session (Fig. 6*D*; Trial, $F_{(13,273)}$ = 7.30, $p < 0.001$; Virus, $F_{(1,21)}$ = 0.19, p = 0.670;

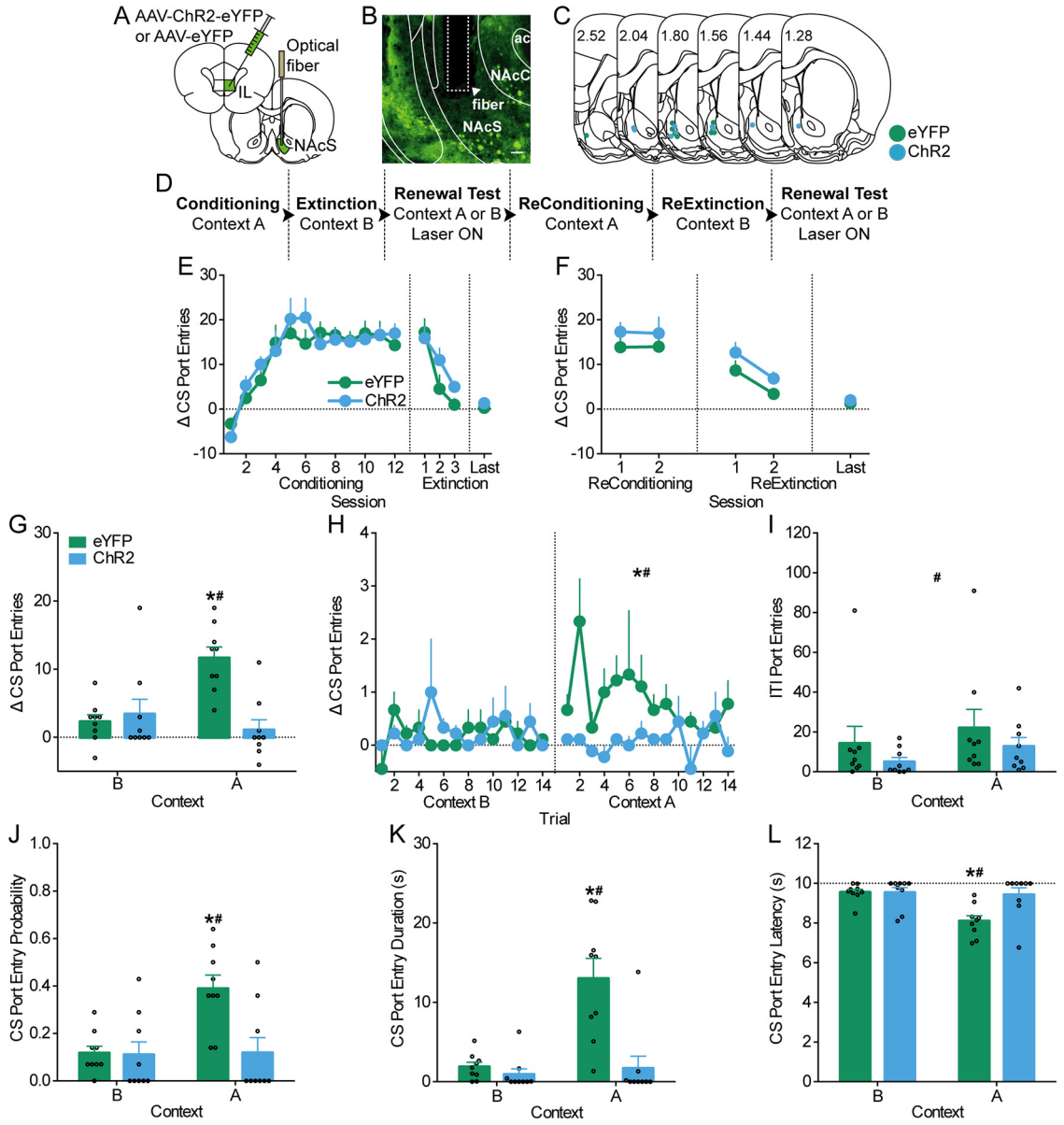

Figure 4. Optogenetic stimulation of the IL-to-NAcS neural circuit suppressed context-induced renewal of appetitive Pavlovian conditioned responding. ***A***, Method schematic of microinjections of ChR2 or eYFP alone in the IL and an optical fiber implanted in the NAcS. ***B***, Representative image depicting ChR2 expression in IL terminals and the optical fiber within the NAcS. ac, Anterior commissure; NAcC, Nucleus accumbens core. Scale bar, 100 µm. ***C***, Optical fiber placements in the NAcS for ChR2-expressing (blue) or eYFP-alone-expressing (green) rats included in the final data analysis. Numbers are locations of sections relative to bregma. ***D***, Design of behavioral procedures. ***E***, ***F***, Δ CS port entries during Conditioning and ReConditioning in Context A and Extinction and ReExtinction in Context B before tests. ***G***, Δ CS port entries at tests in the conditioning context (Context A) for renewal compared to the extinction context (Context B); *$p < 0.05$ ChR2 versus eYFP in Context A; #$p < 0.05$ Context A versus Context B in the eYFP group. ***H***, Δ CS port entries across trials at tests in Context A for renewal and the extinction context, Context B; *$p < 0.05$ ChR2 versus eYFP in Context A across trials; #$p < 0.05$ Context A versus Context B in the eYFP group across trials. ***I***, ITI port entries during tests in Context A and Context B; # $p < 0.05$ main effect of context. ***J–L***, Probability (***J***), duration (***K***), and latency (***L***) of CS port entries during the renewal test in Context A compared to test in the extinction context, Context B. Dashed line indicates duration of the CS and maximum latency (***L***); *$p < 0.05$ ChR2 versus eYFP in Context A; #$p < 0.05$ Context A versus Context B in the eYFP group. All data indicate mean ± SEM.

Trial × Virus, $F_{(13,273)} = 0.66$, $p = 0.760$). Δ CS port entries were equivalent for all virus and extinction groups during the Pavlovian reconditioning session to re-establish baseline responding (Virus, $F_{(1,41)} = 0.02$, $p = 0.881$; Group, $F_{(1,41)} = 0.18$, $p = 0.675$; Virus × Group, $F_{(1,41)} = 0.67$, $p = 0.417$).

In test 1, optogenetic stimulation of the IL-to-NAcS neural circuit during CS trials suppressed Δ CS port entries in the ChR2 groups compared to the eYFP groups regardless of prior extinction training (Fig. 6*E*; Virus, $F_{(1,41)} = 18.32$, $p < 0.001$; Group, $F_{(1,41)} = 3.80$, $p = 0.058$; Virus × Group, $F_{(1,41)} = 0.02$, $p = 0.890$). Δ CS port entries decreased across trials within the test but were overall greater in the eYFP groups compared to the ChR2 groups (Fig. 6*F*; Trial, $F_{(13,533)} = 10.71$, $p < 0.001$; Virus, $F_{(1,41)} = 18.32$, $p < 0.001$; Group, $F_{(1,41)} = 3.80$, $p = 0.058$; Virus × Group, $F_{(1,41)} = 0.02$, $p = 0.890$). There was no statistically significant interaction among trial, virus, and group (Trial × Virus, $F_{(13,533)} = 1.66$, $p = 0.109$; Trial × Group, $F_{(13,533)} = 1.04$, $p = 0.404$, Trial × Virus × Group, $F_{(13,533)} = 1.45$, $p = 0.179$). ITI port entries were equivalent across all groups during test 1 (data not shown; Virus, $F_{(1,41)} = 0.91$, $p = 0.346$; Group, $F_{(1,41)} = 0.05$, $p = 0.829$; Virus × Group, $F_{(1,41)} = 0.18$, $p = 0.671$).

Additional measures during test 1 further support that IL-to-NAcS stimulation during CS trials suppressed conditioned

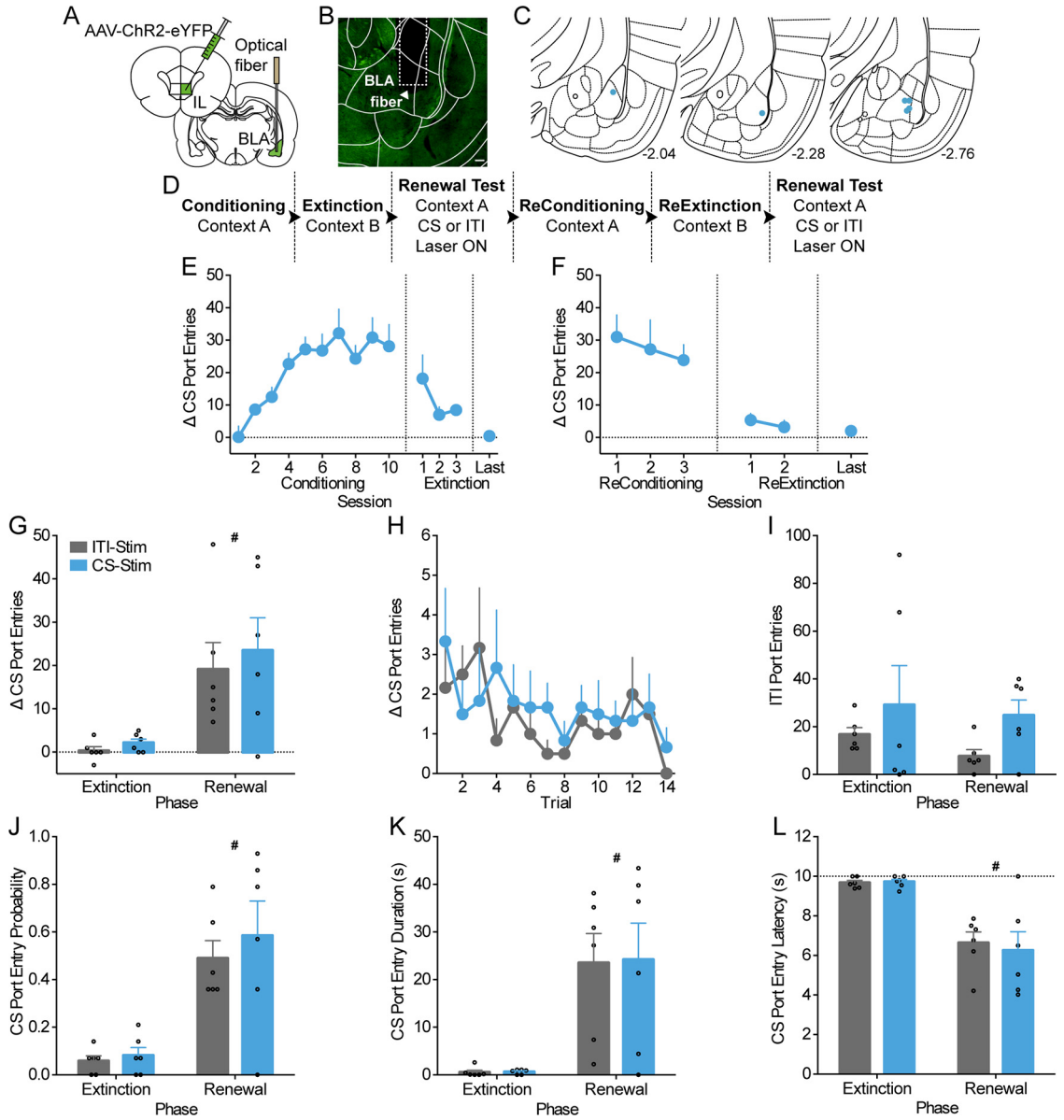

Figure 5. Optogenetic stimulation of the IL-to-BLA neural circuit did not affect context-induced renewal of appetitive Pavlovian conditioned responding. ***A***, Method schematic of microinjections of ChR2 in the IL and an optical fiber implanted in the BLA. ***B***, Representative image depicting ChR2 expression in IL terminals and the optical fiber within the BLA. Scale bar, 100 μm. ***C***, Optical fiber placements in the BLA for ChR2-expressing rats included in the final data analysis. Numbers are locations relative to bregma. ***D***, Design of behavioral procedures. ***E***, ***F***, Δ CS port entries during Conditioning and ReConditioning in Context A and Extinction and ReExtinction in Context B. ***G***, Δ CS port entries during the last session of Extinction in Context B and the Renewal tests in Context A with optogenetic stimulation delivered either during the CS or the middle of the ITI. ***H***, Δ CS port entries across trials during the Renewal tests. ***I***, ITI port entries during the last session of Extinction and the Renewal tests. ***J–L***, Probability (***J***), duration (***K***), and latency (***L***) of CS port entries during the last session of Extinction and the Renewal tests; #$p < 0.05$ main effect of phase. All data indicate mean ± SEM.

responding regardless of extinction (Fig. 6*I–K*, left). Probability of CS port entries were attenuated in the ChR2 groups compared to the eYFP groups regardless of prior extinction training (Fig. 6*I*, left; Virus, $F_{(1,41)} = 17.08$, $p < 0.001$; Group, $F_{(1,41)} = 1.61$, $p = 0.211$; Virus × Group, $F_{(1,41)} = 0.002$, $p = 0.961$). Duration of CS port entries were lower in ChR2 groups compared to the eYFP groups (Fig. 6*J*, left; Virus, $F_{(1,41)} = 36.26$, $p < 0.001$) and were lower in the Extinction groups compared to the No Extinction groups (Group, $F_{(1,41)} = 9.15$, $p = 0.004$) with no statistically significant interaction (Virus × Group, $F_{(1,41)} = 0.69$, $p = 0.412$). Finally, latency to initiate a CS port entry was greater in the ChR2 group compared to the eYFP group regardless of prior extinction training (Fig. 6*K*, left; Virus, $F_{(1,41)} = 7.19$, $p = 0.011$; Group, $F_{(1,41)} = 0.86$, $p = 0.360$; Virus × Group, $F_{(1,41)} = 0.21$, $p = 0.651$).

Together, optogenetic stimulation of the IL-to-NAcS circuit suppressed appetitive Pavlovian conditioned responding during test 1 regardless of prior extinction training and did so from the very first trial.

IL-to-NAcS stimulation during extinction did not facilitate extinction retrieval of appetitive Pavlovian conditioned responding

We conducted another extinction session (test 2) the following day in the absence of optogenetic stimulation to determine whether prior stimulation of the IL-to-NAcS neural circuit would facilitate extinction retrieval of appetitive Pavlovian conditioned responding. This prediction was based on findings in aversive Pavlovian conditioning studies in which stimulation of

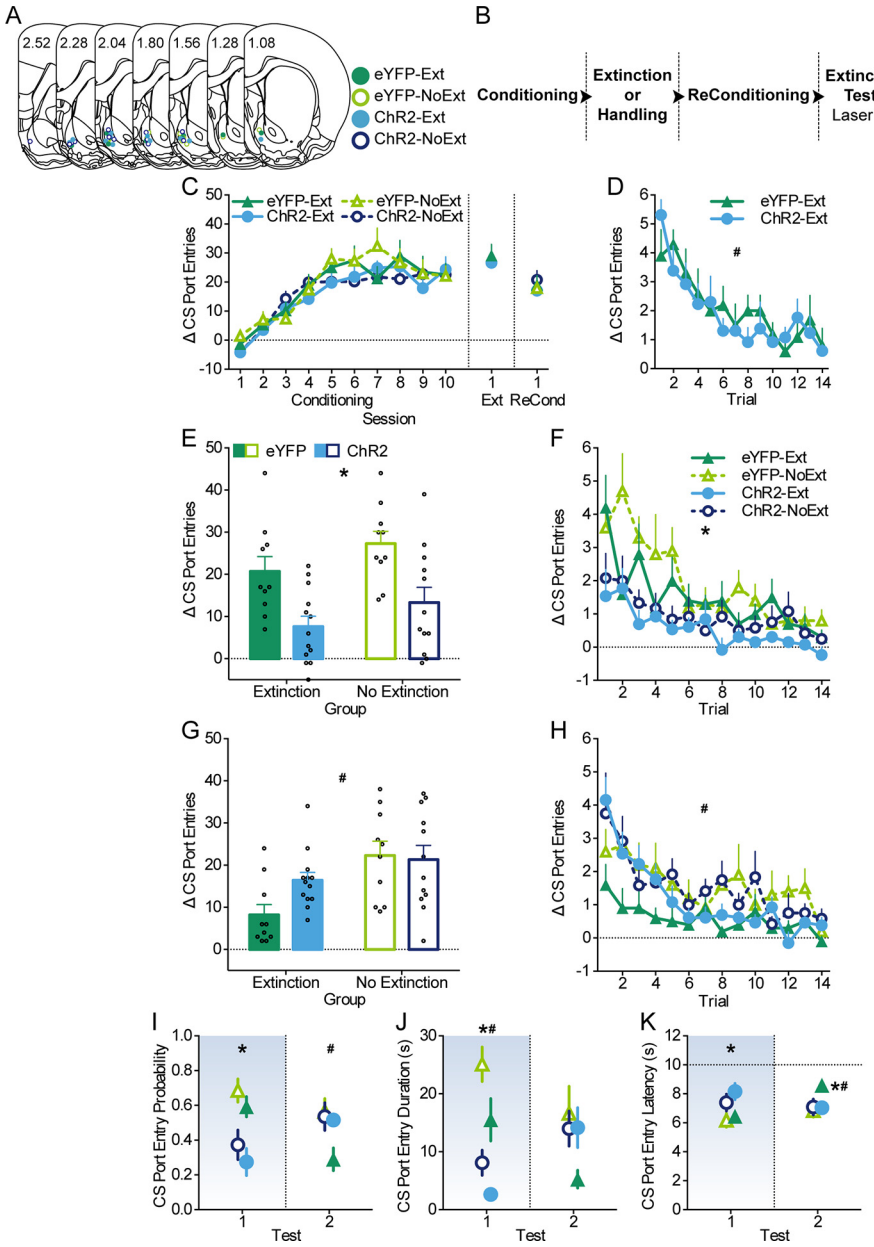

Figure 6. Optogenetic stimulation of the IL-to-NAcS neural circuit suppressed Δ CS port entries regardless of prior extinction and did not facilitate extinction retrieval. ***A***, Optical fiber placements in the NAcS of rats expressing either ChR2 (blue) or eYFP alone (green) in the Extinction (filled) or No Extinction (open) group included in the final data analysis. Numbers are locations of sections relative to bregma. ***B***, Design of behavioral procedures. ***C***, Δ CS port entries across Conditioning, Extinction (Ext), and ReConditioning (ReCond) sessions. ***D***, Δ CS port entries across trials in the extinction session of rats in the Extinction group; #$p < 0.05$ main effect of trial. ***E***, Δ CS port entries during the extinction test (test 1) with IL-to-NAcS stimulation during CS trials. ***F***, Δ CS port entries across trials during the extinction test (test 1) with IL-to-NAcS stimulation during the CS; *$p < 0.05$ main effect of virus group (***E***, ***F***). ***G***, Δ CS port entries during the extinction retrieval test (test 2) without IL-to-NAcS stimulation. ***H***, Δ CS port entries across trials during the extinction retrieval test (test 2) without IL-to-NAcS stimulation; #$p < 0.05$ main effect of extinction group (***G***, ***H***). ***I–K***, Probability (***I***), duration (***J***), and latency (***K***) of CS port entries during the extinction test (test 1) with optogenetic stimulation during CS trials (shaded), and the extinction retrieval test (test 2) without optogenetic stimulation; *$p < 0.05$ main effect of virus group, #$p < 0.05$ main effect of extinction group (***I***, ***J***). ***K***, Test 1, *$p < 0.05$ main effect of virus group; test 2, *$p < 0.05$ ChR2 versus eYFP in the extinction group, #$p < 0.05$ extinction versus no extinction in the eYFP group. Horizontal dashed line indicates duration of the CS and maximum latency. All data indicate mean ± SEM.

the IL during extinction facilitated subsequent extinction retrieval (Milad and Quirk, 2002; Milad et al., 2004; Do-Monte et al., 2015; Lingawi et al., 2017, 2018).

In test 2, Δ CS port entries were lower in rats that received prior extinction training compared to the No Extinction group (Fig. 6*G*; Group, $F_{(1,41)} = 8.71$, $p = 0.005$) with no differences between ChR2 and eYFP groups (Virus, $F_{(1,41)} = 1.75$, $p = 0.193$). There was a near-significant interaction (Virus × Group, $F_{(1,41)} = 3.24$, $p = 0.079$), supporting a possible effect of prior IL-to-NAcS stimulation on extinction retrieval. Exploratory simple effect comparisons showed a significant difference between ChR2 and eYFP groups within the Extinction group ($F_{(1,41)} = 4.97$, $p = 0.031$) but not in the No Extinction group ($F_{(1,41)} = 0.11$, $p = 0.740$). Visual inspection of Figure 6*G* shows that within the Extinction group, Δ CS port entries were higher in the ChR2 group than in the eYFP group, suggesting impaired extinction retrieval in the ChR2 Extinction group. Furthermore, Δ CS port entries were lowest in the eYFP group, which had previously received extinction compared with all other groups.

Δ CS port entries decreased across trials (Fig. 6*H*; Trial, $F_{(13,533)} = 9.06$, $p < 0.001$) but was greater in the No Extinction group compared to the Extinction group (Group, $F_{(1,41)} = 11.33$, $p = 0.002$) with no effect of virus (Virus, $F_{(1,41)} = 1.63$, $p = 0.209$, Virus × Group, $F_{(1,41)} = 2.61$, $p = 0.114$). This effect was largely mediated by the difference in the eYFP Extinction and eYFP No Extinction groups, as both ChR2 groups performed similarly across trials. There were no statistically significant interactions among trial, virus, and group (Trial × Virus, $F_{(13,533)} = 1.55$, $p = 0.122$; Trial × Group, $F_{(13,533)} = 0.50$, $p = 0.888$; Trial × Virus × Group, $F_{(13,533)} = 0.92$, $p = 0.517$). Exploratory analysis comparing ChR2 and eYFP Extinction groups alone revealed that the ChR2 group made significantly more Δ CS port entries than the eYFP group at test 2 (Virus, $F_{(1,21)} = 7.19$, $p = 0.014$). Δ CS port entries decreased across Trial ($F_{(13,273)} = 7.22$, $p < 0.001$), with a significant Trial × Virus interaction ($F_{(13,273)} = 2.31$, $p = 0.020$). Additional *post hoc* analysis indicates that within the extinction group, Δ CS port entries were higher in the ChR2 group than in the eYFP group in Trial 1 (ChR2 vs eYFP, $p = 0.013$).

ITI port entries were not affected by prior optogenetic stimulation of the IL-to-NAcS circuit and was equivalent across all groups during extinction retrieval (data not shown; Virus, $F_{(1,41)} = 0.06$, $p = 0.803$; Group, $F_{(1,41)} = 0.28$, $p = 0.597$; Virus × Group, $F_{(1,41)} = 1.34$, $p = 0.254$).

Additional measures of conditioned responding indicate that optogenetic stimulation of the IL-to-NAcS during extinction did not facilitate extinction retrieval in the Extinction or No Extinction groups (Fig. 6*I–K*, right). Probability of CS port entries during extinction retrieval was lower in Extinction groups compared to the No Extinction groups (Fig. 6*I*, right; Virus, $F_{(1,41)} = 2.20$, $p = 0.145$; Group, $F_{(1,41)} = 4.89$, $p = 0.033$; Virus × Group, $F_{(1,41)} = 3.68$, $p = 0.062$). Visual inspection suggests that this effect was largely driven by lower probability of CS port entries in eYFP Extinction group compared with the eYFP No Extinction group. The ChR2 Extinction and ChR2 No Extinction groups had similar probability of CS port entries during extinction retrieval. Duration of CS port entries was similar across all groups during extinction retrieval (Fig. 6*J*, right; Virus, $F_{(1,41)} = 0.86$, $p = 0.358$; Group, $F_{(1,41)} = 2.73$, $p = 0.106$; Virus × Group, $F_{(1,41)} = 2.88$, $p = 0.097$). Visual inspection indicates, however, that the eYFP Extinction group had lower CS port entry durations than the eYFP No Extinction group, whereas the ChR2 Extinction and ChR2 No Extinction groups had similar duration of CS port entries during extinction retrieval. Within the Extinction group, the ChR2 group showed higher duration of CS port entries compared to the eYFP group. IL-to-NAcS stimulation during extinction impaired subsequent extinction retrieval as measured by average latency to initiate a CS port entry in rats that previously received extinction training (Fig. 6*K*, right; Virus, $F_{(1,41)} = 2.19$, $p = 0.146$; Group, $F_{(1,41)} = 3.83$, $p = 0.057$; Virus × Group, $F_{(1,41)} = 4.22$, $p = 0.046$). The eYFP Extinction group had longer CS port entry latency than the eYFP No Extinction group during extinction retrieval ($p = 0.010$). CS port entry latency was similar between ChR2 and eYFP No Extinction groups ($p = 0.690$) and between ChR2 Extinction and ChR2 No Extinction groups ($p = 0.943$). Within the Extinction groups, the eYFP group had longer CS port entry latency compared to the ChR2 group ($p = 0.016$), suggesting that prior IL-to-NAcS stimulation during extinction impaired subsequent extinction retrieval.

Together, these results suggest that prior IL-to-NAcS stimulation did not facilitate extinction retrieval, and exploratory analyses suggest that stimulation may have instead impaired extinction retrieval in rats that previously received extinction training.

IL-to-NAcS circuit stimulation did not prevent the acquisition of Pavlovian conditioned responding

Experiment 3 tested whether IL-to-NAcS stimulation during CS trials would lead to general response inhibition and prevent the acquisition of appetitive Pavlovian conditioning. During conditioning, the US was initiated 4 s after CS onset. Therefore, we analyzed the effect of IL-to-NAcS stimulation on a CS-only interval consisting of the first 4 s after CS onset, as well as on a 6 s interval encompassing the CS and US during conditioning. A Δ CS-only port entry score was calculated by subtracting port entries made 4 s before CS onset from port entries made during the 4 s CS-only interval. Δ CS-only port entries increased equivalently across conditioning sessions in both the ChR2 and eYFP group (Fig. 7*C*; Session, $F_{(11,220)} = 24.56$, $p < 0.001$; Virus, $F_{(1,20)} = 2.70$, $p = 0.116$, Session × Virus, $F_{(11,220)} = 0.65$, $p = 0.675$). Port entries made during the remaining 6 s combining the CS and US interval were not affected by IL-to-NAcS stimulation (Fig. 7*D*; Session, $F_{(11,220)} = 5.55$, $p < 0.001$; Virus, $F_{(1,20)} = 3.45$, $p = 0.078$, Session × Virus, $F_{(11,220)} = 1.75$, $p = 0.143$). The trending main effect of virus is likely because of the reduced number of port entries in sessions 6–8 of Pavlovian conditioning in the ChR2 group. Interestingly, post CS port entries (10 s interval after CS offset) were greater in the ChR2 group compared to the eYFP group during Pavlovian conditioning (Fig. 7*E*; Session, $F_{(11,220)} = 3.49$, $p = 0.007$; Virus, $F_{(1,20)} = 16.08$, $p = 0.001$; Session × Virus, $F_{(11,220)} = 1.96$, $p = 0.097$).

ITI port entries were similar between ChR2 and eYFP groups during Pavlovian conditioning (Figs. 7*I*, left; Session, $F_{(11,220)} = 14.75$, $p < 0.001$; Virus, $F_{(1,20)} = 2.81$, $p = 0.109$; Session × Virus, $F_{(11,220)} = 1.07$, $p = 0.385$). IL-to-NAcS stimulation decreased the probability (Fig. 7*J*, left; Session, $F_{(11,220)} = 44.51$, $p < 0.001$; Virus, $F_{(1,20)} = 4.49$, $p = 0.047$; Session × Virus, $F_{(11,220)} = 1.14$, $p = 0.342$) but did not affect the duration of CS-only port entries during conditioning (Fig. 7*K*, left; Session, $F_{(11,220)} = 37.78$, $p < 0.001$; Virus, $F_{(1,20)} = 1.87$, $p = 0.187$; Session × Virus, $F_{(11,220)} = 1.53$, $p = 0.224$). IL-to-NAcS stimulation increased the latency (Fig. 7*L*, left; Session, $F_{(11,220)} = 42.18$, $p < 0.001$; Virus, $F_{(1,20)} = 6.73$, $p = 0.017$; Session × Virus, $F_{(11,220)} = 2.03$, $p = 0.083$) of CS-only port entries in the ChR2 group compared to the eYFP group during conditioning.

In sum, IL-to-NAcS stimulation did not prevent acquisition of appetitive Pavlovian conditioned responding but may have affected other aspects of CS responding and increased Post CS port entries.

IL-to-NAcS stimulation was required for the expression of appetitive Pavlovian conditioned responding

Following conditioning, rats were tested in counterbalanced order for the expression of appetitive Pavlovian conditioned responding under extinction conditions. At test, removing optogenetic stimulation abolished Δ CS port entries in the ChR2 group but not the eYFP group (Fig. 7*F*; Test, $F_{(1,20)} = 7.62$, $p = 0.012$; Virus, $F_{(1,20)} = 2.89$, $p = 0.105$; Test × Virus, $F_{(1,20)} = 11.97$, $p = 0.002$). The eYFP group displayed an equivalent high number of Δ CS port entries at test in the presence (Stimulation) or absence (No Stimulation) of stimulation ($p = 0.626$). In contrast, the ChR2 group had more Δ CS port entries when IL-to-NAcS stimulation was present during the CS compared with when stimulation was removed ($p < 0.001$). In the presence of IL-to-NAcS stimulation, there was no statistically significant

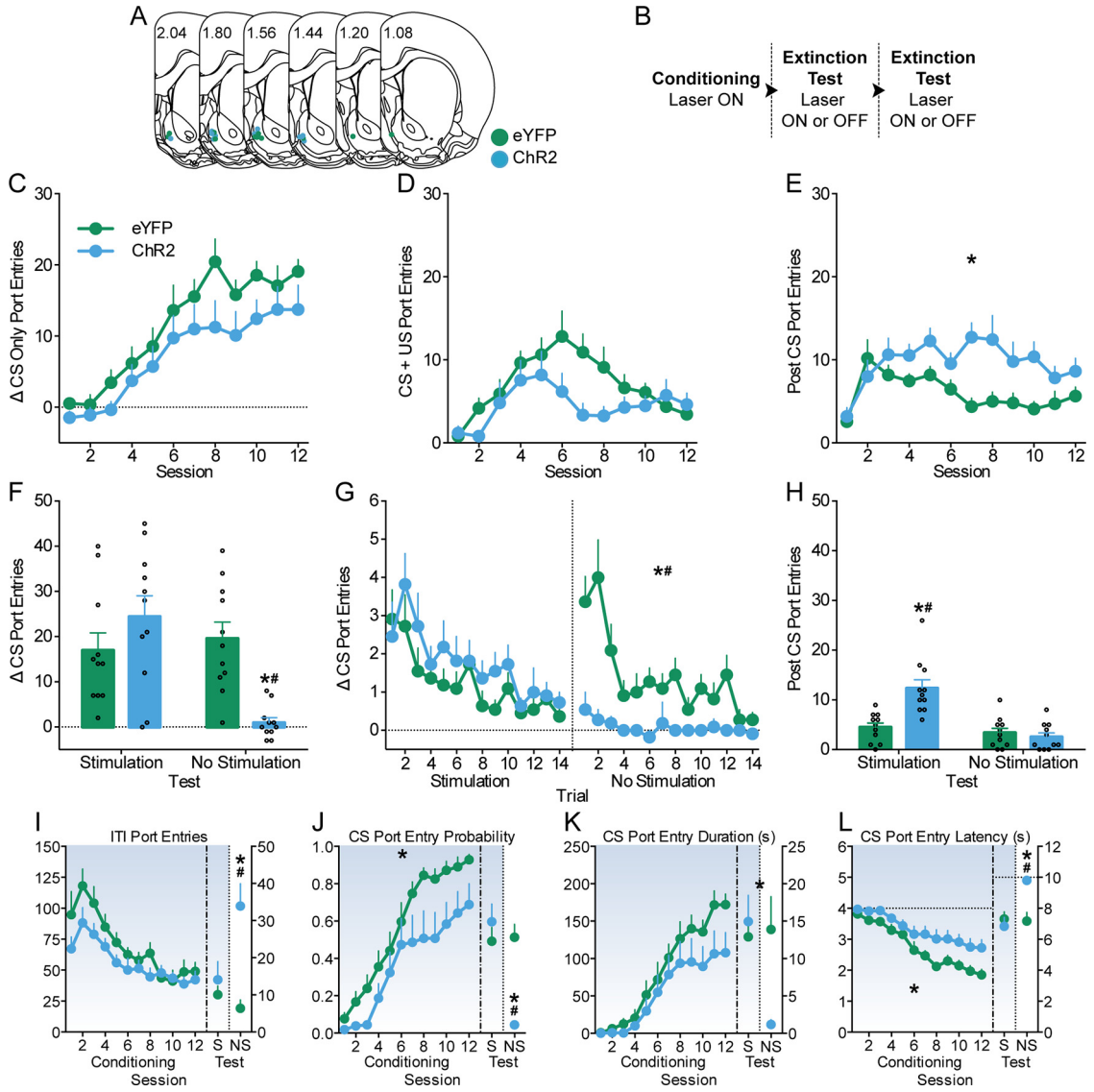

Figure 7. Optogenetic stimulation of the IL-to-NAcS neural circuit altered Pavlovian conditioning. ***A***, Optical fiber placements in the NAcS of rats expressing either ChR2 (blue) or eYFP alone (green) included in the final data analysis. Numbers are locations of sections relative to bregma. ***B***, Design of behavioral procedures. ***C***, Δ CS only port entries (4 s) across Pavlovian conditioning sessions with IL-to-NAcS stimulation during CS trials. ***D***, Port entries during the 6 s overlapping CS and US interval across Pavlovian conditioning sessions. ***E***, Post CS port entries across Pavlovian conditioning sessions; $*p < 0.05$ main effect of virus group. ***F***, Δ CS port entries during the expression test under extinction conditions in the presence (Stimulation) or absence (No Stimulation) of IL-to-NAcS optogenetic stimulation during the CS. ***G***, Δ CS port entries across trials in the Stimulation and No Stimulation expression tests.$*p < 0.05$ ChR2 versus eYFP in the No Stimulation test, $\#p < 0.05$ Stimulation test versus No Stimulation test in the ChR2 group (***F–G***). ***H***, Post CS port entries during the Stimulation and No Stimulation expression tests; $*p <$ 0.05 ChR2 versus eYFP in the Stimulation test, $\#p < 0.05$ Stimulation test versus No Stimulation test in the ChR2 group. ***I***, ITI port entries across Pavlovian conditioning sessions and the expression tests with Stimulation (S) or No Stimulation (NS) under extinction conditions. ***J–L***, Probability (***J***), duration (***K***), and latency (***L***) of CS-only port entries (4 s) across Pavlovian conditioning sessions (left) and full CS port entries (10 s) during the expression tests (right). ***I–L***, Left, The *y*-axis is for data during Pavlovian conditioning. Right, The *y*-axis is for data during the expression tests. Shaded regions indicate sessions in which optogenetic stimulation was present during the CS. Horizontal dashed lines indicate maximum latency. During Pavlovian conditioning, $*p <$ 0.05 main effect of virus. ***I***, ***J***, ***L***, During tests, $*p < 0.05$ ChR2 versus eYFP in the No Stimulation test, $\#p < 0.05$ Stimulation test versus No Stimulation test in the ChR2 group. ***K***, During tests, $*p < 0.05$ main effect of virus. All data indicate mean ± SEM.

difference in Δ CS port entries between the ChR2 and eYFP groups ($p = 0.229$). However, the ChR2 group made fewer port entries than the eYFP group at test when stimulation was removed ($p < 0.001$).

Analysis of Δ CS port entries per CS trial revealed that removing IL-to-NAcS stimulation abolished responding to the CS from the first trial and onward in the ChR2 group (Figure 7*G*; Test, $F_{(1,20)} = 7.62$, $p = 0.012$; Virus, $F_{(1,20)} = 2.89$, $p = 0.105$); Test × Virus, $F_{(1,20)} = 11.97$, $p = 0.002$). This result recapitulates the differences observed in averaged Δ CS port entries between ChR2 and eYFP groups. Within-session extinction was observed as Δ CS port entries decreased across CS trials (Trial, $F_{(13,260)} = 10.07$, $p < 0.001$). However, there were no statistically significant Trial × Virus ($F_{(13,260)} = 1.345$, $p = 0.224$), Trial × Test ($F_{(13,260)} = 0.89$, $p = 0.540$) or Trial × Test × Virus ($F_{(13,260)} = 1.88$, $p = 0.050$) interactions. The near-significant Trial × Test × Virus interaction is likely the result of a reduction in the number of Δ CS port entries, especially in earlier CS trials, in the ChR2 group compared to the eYFP group when stimulation was removed. In contrast, Δ CS port entries underwent within-session extinction and decreased equivalently across trials in both the eYFP group and the ChR2 group when stimulation was present during CS trials.

The presence of optogenetic stimulation increased Post CS port entries in the ChR2 group but not in the eYFP group during the expression tests (Figure 7*H*; (Test, $F_{(1,20)} = 22.32$, $p < 0.001$; Virus, $F_{(1,20)} = 10.35$, $p = 0.004$; Test × Virus, $F_{(1,20)} = 14.28$, $p = 0.001$). The eYFP group displayed similarly low Post CS port entries at test in the presence or absence of stimulation ($p = 0.512$). In contrast, the ChR2 group made more Post CS port entries during the Stimulation test than the No Stimulation test ($p < 0.001$). The ChR2 group made more Post CS port entries than the eYFP group during the Stimulation test ($p < 0.001$) but not in the No Stimulation test ($p = 0.510$).

At test, removing optogenetic stimulation increased ITI port entries in the ChR2 group but not in the eYFP group (Fig. 7*I*, right; Test, $F_{(1,20)} = 5.20$, $p = 0.034$; Virus, $F_{(1,20)} = 10.84$, $p = 0.004$; Test × Virus, $F_{(1,20)} = 11.14$, $p = 0.003$). The eYFP group showed an equivalent number of ITI port entries in the presence or absence of optogenetic stimulation ($p = 0.464$). In contrast, removing IL-to-NAcS stimulation in the ChR2 group increased ITI port entries compared to when stimulation was present ($p = 0.001$). The ChR2 group made more ITI port entries than the eYFP group during the No Stimulation test ($p < 0.001$) but similar ITI port entries during the Stimulation test ($p = 0.468$).

Additional measures support that removal of IL-to-NAcS stimulation at test abolished conditioned responding in the ChR2 group but not the eYFP group (Fig. 7*J–L*, right). Removal of optogenetic stimulation abolished probability of CS port entries in the ChR2 group but not in the eYFP group (Fig. 7*J*, right; Test, $F_{(1,20)} = 15.08$, $p = 0.001$; Virus, $F_{(1,20)} = 6.42$, $p = 0.020$; Test × Virus, $F_{(1,20)} = 17.43$, $p < 0.001$). The eYFP maintained high probability of CS port entries in the Stimulation and No Stimulation tests ($p = 0.839$). In contrast, the ChR2 group had lower probability of CS port entries during the No Stimulation test compared to the Stimulation test ($p < 0.001$). The ChR2 had lower probability of CS port entries than the eYFP group during the No Stimulation test ($p < 0.001$) but similar CS port entry probabilities during the Stimulation test ($p = 0.397$). Duration of CS port entries was lower at test in the ChR2 group compared with the eYFP group (Fig. 7*K*, right; Test, $F_{(1,20)} = 2.76$, $p = 0.113$; Virus, $F_{(1,20)} = 4.49$, $p = 0.047$; Test × Virus, $F_{(1,20)} = 3.69$, $p = 0.069$). Visual inspection suggests that this effect may have largely been driven by lower duration of CS port entries in the ChR2 group compared to the eYFP group during the No Stimulation test. Removal of optogenetic stimulation increased the latency of CS port entries in the ChR2 group but not in the eYFP group (Fig. 7*L*, right; Test, $F_{(1,20)} = 9.94$, $p = 0.005$, Virus, $F_{(1,20)} = 4.72$, $p = 0.042$; Test × Virus, $F_{(1,20)} = 11.95$, $p = 0.002$). The eYFP group maintained similarly short latency of CS port entries during the Stimulation and No Stimulation tests ($p = 0.831$). In contrast, the ChR2 group had longer latency of CS port entries during the No Stimulation test compared to the Stimulation test ($p < 0.001$). The ChR2 group had longer latency of CS port entries than the eYFP group during the No Stimulation test ($p < 0.001$) but similar latency of CS port entries during the Stimulation test ($p = 0.533$).

In sum, removing IL-to-NAcS stimulation reduced Δ CS port entries in the ChR2 group without affecting conditioned responding in the eYFP group. Further, removing IL-to-NAcS stimulation increased port entries made during the ITI in the ChR2 group without affecting responding in the eYFP group.

Discussion

We report that optogenetically stimulating the IL-to-NAcS neural circuit during CS trials suppressed context-induced renewal of appetitive Pavlovian conditioned responding without affecting responding in the extinction context or outside CS trials. In contrast, optogentically stimulating the IL-to-BLA circuit did not affect context-induced renewal. Further, IL-to-NAcS stimulation suppressed conditioned responding regardless of prior extinction and seemed to impair extinction retrieval. Finally, IL-to-NAcS stimulation altered but did not prevent the acquisition of Pavlovian conditioning and was necessary to maintain subsequent expression of conditioned responding. These results suggest that stimulating the IL-to-NAcS circuit suppresses responding to appetitive Pavlovian cues, and this effect does not require prior extinction.

As predicted, in experiment 1, IL-to-NAcS stimulation during CS trials suppressed the renewal of conditioned responding. Suppression occurred in the first CS trial at test in Context A and was reflected in additional measures of conditioned responding. These results are consistent with the proposed role of the IL in suppressing appetitive Pavlovian responses (Rhodes and Killcross, 2004, 2007; Villaruel et al., 2018) and with evidence that IL inputs to the NAcS are critical for suppressing operant cocaine-seeking (Peters et al., 2008, 2009; LaLumiere et al., 2012; Augur et al., 2016; Cameron et al., 2019; Warren et al., 2019). Our results extend these findings to appetitive Pavlovian responses using sucrose, a natural reinforcer. Therefore, the suppression of Pavlovian responding to appetitive cues and operant cocaine-seeking after extinction may be mediated by a common neural substrate.

Experiment 2 tested whether IL-to-NAcS stimulation suppressed renewal by promoting the expression of an inhibitory extinction memory. Thus, following Pavlovian conditioning, rats received either extinction training or no extinction before test. Optogenetically stimulating the IL-to-NAcS circuit at test suppressed CS responding regardless of prior extinction. Therefore, the suppression of renewal in experiment 1 following IL-to-NAcS stimulation may have been accomplished through an extinction-independent process. However, it is important to note that conditioning and extinction were conducted in different contexts in experiment 1, but the same context in experiment 2, which could alter how the CS undergoes extinction (Delamater and Westbrook, 2014). These results are inconsistent with the hypothesis that IL and IL-to-NAcS circuit stimulation suppresses operant cocaine-seeking by promoting extinction retrieval (Peters et al., 2008; Augur et al., 2016; Müller Ewald et al., 2019). This discrepancy could be related to our use of Pavlovian conditioning, whereas studies investigating the IL-to-NAcS circuit in extinction typically use operant cocaine self-administration. Differences in the associations involved during extinction of Pavlovian versus operant responding have been proposed (Trask et al., 2017), which could also influence the recruitment of the IL-to-NAcS circuit.

Alternatively, studies in operant cocaine-seeking used chemogenetics and stable-step function opsins to diffusely enhance IL and IL-to-NAcS activity (Augur et al., 2016; Müller Ewald et al., 2019), whereas we used optogenetics to stimulate the IL-to-NAcS circuit at discrete points during behavior. Similar application of optogenetics to stimulate the IL and IL-to-NAcS circuit suppressed operant responding for food and cocaine without prior extinction (Do-Monte et al., 2015; Cameron et al., 2019). Optogenetic stimulation of IL inputs in the NAcS may disrupt time-locked inhibitory activity in the NAcS that permits consummatory behaviors (Nicola et al., 2004; Taha and Fields, 2006; Krause et al., 2010; Reed et al., 2018), which is a component of the CS-elicited port entry response in our task.

The IL mediates inhibitory associations established through latent inhibition, wherein pre-exposure to a nonreinforced CS delays the subsequent acquisition of Pavlovian conditioning (Lingawi et al., 2017). In our task, exposure to a nonreinforced CS, and therefore the establishment of inhibitory associations through latent inhibition, may have occurred early in conditioning as rats were first learning to enter the fluid port during the CS to obtain sucrose. Pharmacologically stimulating the IL strengthens inhibitory associations acquired through latent inhibition (Lingawi et al., 2017). Therefore, optogenetically stimulating the IL-to-NAcS circuit could potentially suppress responding regardless of prior extinction by facilitating the expression of inhibitory associations established early in Pavlovian conditioning through latent inhibition.

Different neural ensembles involved in promoting and suppressing operant responding have been identified in the IL and IL projections to the NAcS (Warren et al., 2016; Warren et al., 2019). Further, pharmacologically inactivating the IL can reduce operant food- and heroin-seeking (Bossert et al., 2012; Eddy et al., 2016), suggesting that the IL is also involved in promoting responding after extinction. Therefore, our global stimulation of the IL-to-NAcS circuit may have disrupted the activity of neural ensembles involved in promoting responding, thereby suppressing appetitive Pavlovian conditioned responding regardless of extinction.

In experiment 2, optogenetically stimulating the IL-to-NAcS circuit during extinction did not facilitate extinction retrieval 24 h later and, in fact, seemed to increase CS responding during the retrieval test in rats with previous extinction training. Therefore, IL-to-NAcS stimulation during extinction seemed to weaken the previously established inhibitory extinction memory. This finding contrasts with studies in aversive conditioning that report facilitated extinction retrieval and strengthening of inhibitory memory after enhancing IL activity during extinction (Milad and Quirk, 2002; Milad, 2004; Do-Monte et al., 2015; Lingawi et al., 2017, 2018). These divergent findings could be because of differences in the affective properties of extinction in aversive and appetitive procedures (Amsel, 1958; Gerber et al., 2014).

Optogenetically stimulating the IL-to-NAcS circuit in experiment 3 did not prevent the acquisition or expression of appetitive Pavlovian conditioning, indicating that this manipulation does not result in general motor inhibition. However, stimulation of this neural circuit affected probability and latency measures of conditioned responding and increased post CS port entries, suggesting that conditioning was altered. Optogenetic stimulation of various glutamatergic inputs into the NAcS including the IL supports self-stimulation (Britt et al., 2012; Cameron et al., 2019), suggesting that stimulating this circuit can generate a perceptible stimulus. Therefore, IL-to-NAcS stimulation in experiment 3 may have generated a predictive stimulus that functioned in compound with the white-noise CS to signal sucrose delivery. Interestingly, IL-to-NAcS stimulation was required for the subsequent expression of responding to the white-noise CS. Removing stimulation decreased CS responding and increased port entries during the ITI. These results suggest that IL-to-NAcS stimulation acted as a predictive cue for sucrose and altered Pavlovian conditioning.

Although ChR2 expression was predominantly in the IL, we observed some spread in the medial orbitofrontal cortex (OFC) and lateral parts of the prelimbic cortex (PL) along the forceps minor of the corpus callosum. Our results could thus be because of optogenetic stimulation of inputs in the NAcS from regions neighboring the IL. However, the PL is thought to promote cocaine-seeking (McFarland and Kalivas, 2001; Capriles et al., 2003; McLaughlin and See, 2003), and optogenetic stimulation of the PL-to-NAc circuit elevates Pavlovian responding (Otis et al., 2017). Furthermore, pharmacologically inactivating the OFC disrupts overexpectation but not extinction in aversive conditioning (Lay et al., 2019). Finally, our findings in experiments 1 and 2 are consistent with numerous studies on the role of the IL and the IL-to-NAcS circuit in extinction using different procedures (Quirk et al., 2000; Milad and Quirk, 2002; Peters et al., 2008; LaLumiere et al., 2012; Augur et al., 2016; Villaruel et al., 2018), suggesting that we successfully targeted the IL-to-NAcS circuit.

We found that IL projections to the NAcS and BLA were largely made up of anatomically distinct neural subpopulations (Bloodgood et al., 2018). Unilateral optogenetic stimulation of the IL-to-NAcS circuit induced bilateral Fos activation in the IL and the NAcS, which may be because of bilateral projections from the IL to the NAcS and contralateral connections between the IL (Hurley et al., 1991; Vertes, 2004). However, Fos activation was greater in the hemisphere transfected with ChR2 and implanted with the optical fiber, suggesting that the IL-to-NAcS circuit is predominantly ipsilateral.

The present research only used male rats, and we were unable to observe sex differences. There are sex differences in the role of the IL in renewal of appetitive Pavlovian conditioned responding (Anderson and Petrovich, 2018a,b). Sex differences in behavioral strategies could lead to differential effects of neural manipulations (Radke et al., 2021; Shansky and Murphy, 2021). We observe similar levels of renewal (Brown and Chaudhri, 2021) and reinstatement (LeCocq and Chaudhri, 2021) of appetitive Pavlovian conditioned responding in male and female rats. Our ongoing research on corticothalamic regulation of extinction investigates potential sex differences (A. Brown and N. Chaudhri, unpublished observations).

In conclusion, optogenetically stimulating the IL-to-NAcS but not the IL-to-BLA circuit suppressed the renewal of appetitive Pavlovian conditioned responding and may have done so in an extinction-independent manner. Additionally, IL-to-NAcS stimulation did not facilitate extinction retrieval, which contrasts with findings in aversive conditioning. Importantly, stimulation of this circuit did not suppress motor function and altered Pavlovian conditioning by potentially acting as a stimulus that became associated with other external stimuli. The present results advance our understanding of the complex processes by which the IL-to-NAcS circuit controls appetitive Pavlovian conditioned responding. Further work is needed in both sexes to determine the mechanisms by which this corticostriatal circuit mediates adaptive behavior. Understanding the corticostriatal mechanisms involved in inhibiting learned responses can aid in the treatment of disorders like substance abuse and post-traumatic stress.

References

Adamantidis AR, Tsai H-C, Boutrel B, Zhang F, Stuber GD, Budygin EA, Touriño C, Bonci A, Deisseroth K, de Lecea L (2011) Optogenetic interrogation of dopaminergic modulation of the multiple phases of reward-seeking behavior. J Neurosci 31:10829–10835.

Amsel A (1958) The role of frustrative nonreward in noncontinuous reward situations. Psychol Bull 55:102–119.

Anderson LC, Petrovich GD (2018a) Distinct recruitment of the hippocampal, thalamic, and amygdalar neurons projecting to the prelimbic cortex in male and female rats during context-mediated renewal of responding to food cues. Neurobiol Learn Mem 150:25–35.

Anderson LC, Petrovich GD (2018b) Ventromedial prefrontal cortex mediates sex differences in persistent cognitive drive for food. Sci Rep 8:2230.

Augur IF, Wyckoff AR, Aston-Jones G, Kalivas PW, Peters J (2016) Chemogenetic activation of an extinction neural circuit reduces cue-induced reinstatement of cocaine-seeking. J Neurosci 36:10174–10180.]

Benn A, Barker GRI, Stuart SA, Roloff EVL, Teschemacher AG, Warburton EC, Robinson ESJ (2016) Optogenetic stimulation of prefrontal glutamatergic neurons enhances recognition memory. J Neurosci 36:4930–4939.

Bloodgood DW, Sugam JA, Holmes A, Kash TL (2018) Fear extinction requires infralimbic cortex projections to the basolateral amygdala. Transl Psychiatry 8:60.

Bossert JM, Stern AL, Theberge FRM, Cifani C, Koya E, Hope BT, Shaham Y (2011) Ventral medial prefrontal cortex neuronal ensembles mediate context-induced relapse to heroin. Nat Neurosci 14:420–422.

Bossert JM, Stern AL, Theberge FRM, Marchant NJ, Wang H-L, Morales M, Shaham Y (2012) Role of projections from ventral medial prefrontal cortex to nucleus accumbens shell in context-induced reinstatement of heroin seeking. J Neurosci 32:4982–4991.

Bouton ME (1993) Context, time, and memory retrieval in the interference paradigms of Pavlovian learning. Psychol Bull 114:80–99.

Bouton ME (2004) Context and behavioral processes in extinction. Learn Mem 11:485–494.

Britt JP, Benaliouad F, McDevitt RA, Stuber GD, Wise RA, Bonci A (2012) Synaptic and behavioral profile of multiple glutamatergic inputs to the nucleus accumbens. Neuron 76:790–803.

Brown A, Chaudhri N, (2021) Activation of a cortico-thalamic neural circuit attenuates renewal in male and female rats. Poster presented at the 30th Annual International Behavioural Neuroscience Society Meeting, Puerto Vallarta, Mexico.

Cameron CM, Murugan M, Choi JY, Engel EA, Witten IB (2019) Increased cocaine motivation is associated with degraded spatial and temporal representations in IL-NAc neurons. Neuron 103:80–91.e7.

Capriles N, Rodaros D, Sorge RE, Stewart J (2003) A role for the prefrontal cortex in stress- and cocaine-induced reinstatement of cocaine-seeking in rats. Psychopharmacology (Berl) 168:66–74.

Delamater AR, Westbrook RF (2014) Psychological and neural mechanisms of experimental extinction: a selective review. Neurobiol Learn Mem 108:38–51.

Do-Monte FH, Manzano-Nieves G, Quiñones-Laracuente K, Ramos-Medina L, Quirk GJ (2015) Revisiting the role of infralimbic cortex in fear extinction with optogenetics. J Neurosci 35:3607–3615.

Eddy MC, Todd TP, Bouton ME, Green JT (2016) Medial prefrontal cortex involvement in the expression of extinction and ABA renewal of instrumental behavior for a food reinforcer. Neurobiol Learn Mem 128:33–39.

Fuchikami M, Thomas A, Liu R, Wohleb ES, Land BB, DiLeone RJ, Aghajanian GK, Duman RS (2015) Optogenetic stimulation of infralimbic PFC reproduces ketamine's rapid and sustained antidepressant actions. Proc Natl Acad Sci U S A 112:8106–8111.

Gerber B, Yarali A, Diegelmann S, Wotjak CT, Pauli P, Fendt M (2014) Pain-relief learning in flies, rats, and man: basic research and applied perspectives. Learn Mem 21:232–252.

Gutman AL, Nett KE, Cosme CV, Worth WR, Gupta SC, Wemmie JA, LaLumiere RT (2017) Extinction of cocaine-seeking requires a window of infralimbic pyramidal neuron activity after unreinforced lever presses. J Neurosci 37:6075–6086.

Hurley KM, Herbert H, Moga MM, Saper CB (1991) Efferent projections of the infralimbic cortex of the rat. J Comp Neurol 308:249–276.

Keistler C, Barker JM, Taylor JR (2015) Infralimbic prefrontal cortex interacts with nucleus accumbens shell to unmask expression of outcome-selective Pavlovian-to-instrumental transfer. Learn Mem 22:509–513.

Konorski J (1948) Conditioned reflexes and neuronal organization. London: Cambridge UP.

Krause M, German PW, Taha SA, Fields HL (2010) A pause in nucleus accumbens neuron firing is required to initiate and maintain feeding. J Neurosci 30:4746–4756.

LaLumiere RT, Smith KC, Kalivas PW (2012) Neural circuit competition in cocaine-seeking: roles of the infralimbic cortex and nucleus accumbens shell. Eur J Neurosci 35:–614–622.

Lay BPP, Nicolosi M, Usypchuk AA, Esber GR, Iordanova MD (2019) Dissociation of appetitive overexpectation and extinction in the infralimbic cortex. Cereb Cortex 29:3687–3701.

LeCocq M, Chaudhri N (2021) The role of u-opioid receptors in the reinstatement of respodning to a cue for alcohol (abstract). Alcohol: *Clin Exp Res*, 45, p151A.

Lingawi NW, Westbrook RF, Laurent V (2017) Extinction and latent inhibition involve a similar form of inhibitory learning that is stored in and retrieved from the infralimbic cortex. Cereb Cortex (New York, NY: 1991)27:5547–5556.

Lingawi NW, Holmes NM, Westbrook RF, Laurent V (2018) The infralimbic cortex encodes inhibition irrespective of motivational significance. Neurobiol Learn Mem 150:64–74.

McFarland K, Kalivas PW (2001) The circuitry mediating cocaine-induced reinstatement of drug-seeking behavior. J Neurosci 21:8655–8663.

McLaughlin J, See RE (2003) Selective inactivation of the dorsomedial prefrontal cortex and the basolateral amygdala attenuates conditioned-cued reinstatement of extinguished cocaine-seeking behavior in rats. Psychopharmacology (Berl) 168:57–65.

Milad MR, Quirk GJ (2002) Neurons in medial prefrontal cortex signal memory for fear extinction. Nature 420:70–74.

Milad MR, Vidal-Gonzalez I, Quirk GJ (2004) Electrical stimulation of medial prefrontal cortex reduces conditioned fear in a temporally specific manner. Behav Neurosci 118:389–394.

Müller R, Bravo R, Burckhardt J, Curran T (1984) Induction of c-*fos* gene and protein by growth factors precedes activation of c-myc. Nature 312:716–720.

Müller Ewald VA, De Corte BJ, Gupta SC, Lillis KV, Narayanan NS, Wemmie JA, LaLumiere RT (2019) Attenuation of cocaine-seeking in rats via enhancement of infralimbic cortical activity using stable step-function opsins. Psychopharmacology (Berl) 236:479–490.

Nicola SM, Yun IA, Wakabayashi KT, Fields HL (2004) Firing of nucleus accumbens neurons during the consummatory phase of a discriminative stimulus task depends on previous reward predictive cues. J Neurophysiol 91:1866–1882.

Otis JM, Namboodiri VMK, Matan AM, Voets ES, Mohorn EP, Kosyk O, McHenry JA, Robinson JE, Resendez SL, Rossi MA, Stuber GD (2017) Prefrontal cortex output circuits guide reward seeking through divergent cue encoding. Nature 543:103–107.

Paxinos G, Watson C (2007) The rat brain in stereotaxic coordinates. New York: Academic.

Pearce JM, Hall G (1980) A model for Pavlovian learning: variations in the effectiveness of conditioned but not of unconditioned stimuli. Psychological Review 87:532–552.

Peters J, LaLumiere RT, Kalivas PW (2008) Infralimbic prefrontal cortex is responsible for inhibiting cocaine-seeking in extinguished rats. J Neurosci 28:6046–6053.

Peters J, Kalivas PW, Quirk GJ (2009) Extinction circuits for fear and addiction overlap in prefrontal cortex. Learn Mem 16:279–288.

Quirk GJ, Mueller D (2008) Neural mechanisms of extinction learning and retrieval. Neuropsychopharmacology 33:56–72.

Quirk GJ, Russo GK, Barron JL, Lebron K (2000) The role of ventromedial prefrontal cortex in the recovery of extinguished fear. J Neurosci 20:6225–6231.

Radke AK, Sneddon EA, Monroe SC (2021) Studying sex differences in rodent models of addictive behavior. Current Protocols 1:1–18.

Reed SJ, Lafferty CK, Mendoza JA, Yang AK, Davidson TJ, Grosenick L, Deisseroth K, Britt JP (2018) Coordinated reductions in excitatory input to the nucleus accumbens underlie food consumption. Neuron 99:1260–1273.e4.

Rhodes SEV, Killcross S (2004) Lesions of rat infralimbic cortex enhance recovery and reinstatement of an appetitive Pavlovian response. Learn Mem 11:611–616.

Rhodes SEV, Killcross AS (2007) Lesions of rat infralimbic cortex enhance renewal of extinguished appetitive Pavlovian responding. Eur J Neurosci 25:2498–2503.

Shansky RM, Murphy AZ (2021) Considering sex as a biological variable will require a global shift in science culture. Nat Neurosci 24:457–464.

Sutton MA, Schmidt EF, Choi K-H, Schad CA, Whisler K, Simmons D, Karanian DA, Monteggia LM, Neve RL, Self DW (2003) Extinction-induced upregulation in AMPA receptors reduces cocaine-seeking behaviour. Nature 421:70–75.

Taha SA, Fields HL (2006) Inhibitions of nucleus accumbens neurons encode a gating signal for reward-directed behavior. J Neurosci 26:217–222.

Trask S, Thrailkill EA, Bouton ME (2017) Occasion setting, inhibition, and the contextual control of extinction in Pavlovian and instrumental (operant) learning. Behav Processes 137:64–72.

Trujillo-Pisanty I, Sanio C, Chaudhri N, Shizgal P (2015) Robust optical fiber patch-cords for in vivo optogenetic experiments in rats. MethodsX 2:263–271.

Vertes RP (2004) Differential projections of the infralimbic and prelimbic cortex in the rat. Synapse 51:32–58.

Vidal-Gonzalez I, Vidal-Gonzalez B, Rauch SL, Quirk GJ (2006) Microstimulation reveals opposing influences of prelimbic and infralimbic cortex on the expression of conditioned fear. Learn Mem 13:728–733.

Villaruel FR, Lacroix F, Sanio C, Sparks DW, Chapman CA, Chaudhri N (2018) Optogenetic activation of the infralimbic cortex suppresses the return of appetitive Pavlovian conditioned responding following extinction. Cereb Cortex 28:4210–4221.

Warren BL, Mendoza MP, Cruz FC, Leao RM, Caprioli D, Rubio FJ, Whitaker LR, McPherson KB, Bossert JM, Shaham Y, Hope BT (2016) Distinct Fos-expressing neuronal ensembles in the ventromedial prefrontal cortex mediate food reward and extinction memories. J Neurosci 36:6691–6703.

Warren BL, Kane L, Venniro M, Selvam P, Quintana-Feliciano R, Mendoza MP, Madangopal R, Komer L, Whitaker LR, Rubio FJ, Bossert JM, Caprioli D, Shaham Y, Hope BT (2019) Separate vmPFC ensembles control cocaine self-administration versus extinction in rats. J Neurosci 39:7394–7407.

Wood M, Adil O, Wallace T, Fourman S, Wilson SP, Herman JP, Myers B (2019) Infralimbic prefrontal cortex structural and functional connectivity with the limbic forebrain: a combined viral genetic and optogenetic analysis. Brain Struct Funct 224: 73–97.